DRF

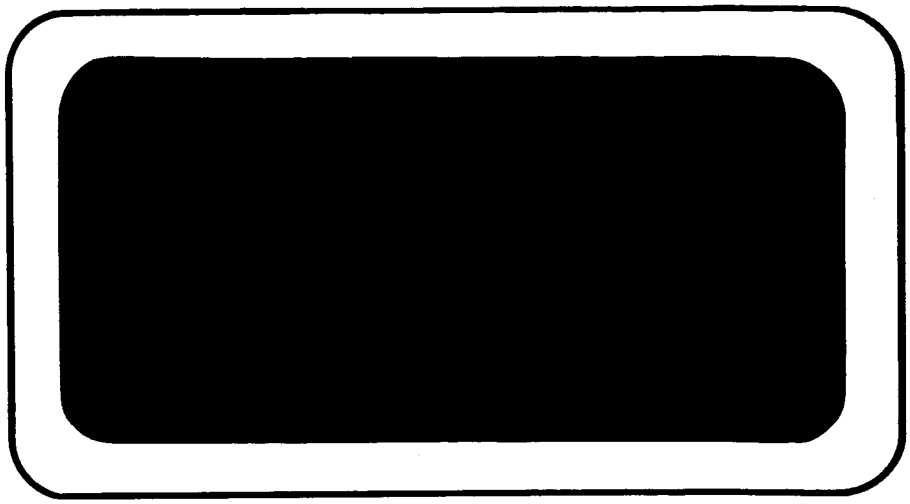

GPO PRICE $ _____

CFSTI PRICE(S) $ _____

Hard copy (HC) 3.00

Microfiche (MF) .75

ff 653 July 65

FACILITY FORM 602

N65-35114 (ACCESSION NUMBER)

63 (PAGES)

CR67282 (NASA CR OR TMX OR AD NUMBER)

1 (THRU)

(CODE)

15 (CATEGORY)

HITTMAN ASSOCIATES, INC. BALTIMORE, MARYLAND

HIT-163

THERMOELECTRIC BONDING STUDY

SUMMARY REPORT

March 1965

Prepared by:
Abraham L. Eiss

Prepared for
National Aeronautics and Space Administration
Goddard Space Flight Center
Greenbelt, Maryland

HITTMAN ASSOCIATES, INC.
BALTIMORE, MARYLAND

LEGAL NOTICE

TABLE OF CONTENTS

		Page
LEGAL NOTICE		ii
TABLE OF CONTENTS		iii
LIST OF TABLES		iv
LIST OF ILLUSTRATIONS		v
FOREWORD		vi
I.	INTRODUCTION AND SUMMARY	1
II.	LITERATURE SURVEY	3
III.	MATERIALS AND EQUIPMENT	5
	A. Materials	5
	B. Equipment	8
IV.	PRELIMINARY BRAZE AND SHOE MATERIAL EVALUATION	14
	A. Preparation of Lead Telluride Elements	14
	B. Selection and Preparation of Braze Alloys	16
	C. Selection of Shoe Materials	20
	D. Wettability Tests	20
V.	POISONING EFFECTS STUDY	25
VI.	BOND PREPARATION AND EVALUATION	33
	A. Bond Preparation	33
	B. Bond Evaluation	35
VII.	STRESS ANALYSIS	39
	A. Thermal Gradient Stress Pattern	39
	B. Shoe Constraint Stress Pattern	42
	C. Torsional Stress Pattern	46
	D. Experimental Program	46
VIII.	REFERENCES	51
APPENDIX A - DERIVATION OF STRESS EQUATIONS		A-1

LIST OF TABLES

Table Number	Title	Page
1	Elemental Metals Purchased for Braze Alloy Preparation	6
2	Prospective Shoe Materials Procured for Testing	7
3	Hot Pressing Conditions for PbTe Thermoelectric Elements	15
4	Room Temperature Electrical Resistivity of PbTe Elements Hot Pressed at Hittman Associates	17
5	Potential Braze Alloys Selected for This Study	19
6	Wettability of PbTe by Braze Materials	21
7	Summary of Wettability Test Results of Brazes on Shoe Materials	24
8	The Effect of Poison Additives on the Seebeck Coefficient and Resistivity of PbTe	27
9	Effects of Aging at 538°C on the Thermoelectric Properties of n-PbTe Containing Additives	32
10	Torque Test Results on Bonded Lead Telluride Thermoelectric Elements	37
11	Torque Test Results on Bonded Lead Telluride Thermoelements Tested After 113 Hours at 538°C	38

LIST OF ILLUSTRATIONS

Figure Number	Title	Page
1	Resistivity Test Apparatus	9
2	Seebeck Test Apparatus	10
3	Plan View of Torsion Test Setup	11
4	Schematic of Wettability Test Setup	12
5	Thermoelectric Bonding Apparatus	13
6	Comparison of Seebeck Coefficient of Hittman Manufactured PbTe with 3M Literature Values	18
7	PbTe Bonded to Iron Shoes with SnTe-Ti Braze	36
8	Thermal Gradient Stress Patterns	40
9	Shoe Constraint Stress Patterns	43
10	Torsional Stress Pattern	47
11	Lead Telluride Thermoelectric Elements Fractured in Torsion	48
12	n-PbTe Thermoelement Tested in Torsion	49

FOREWORD

This report covers the work accomplished during the Thermoelectric Bonding Study performed for the National Aeronautics and Space Administration, Goddard Space Flight Center, under Contract NAS5-3973.

I. INTRODUCTION AND SUMMARY

Lead telluride thermoelectric elements have been used in most thermoelectric power generation devices built and proposed for construction in recent years because of their superior figure of merit in the 100° to 600°C temperature range. For the same reason lead telluride is potentially attractive for several NASA applications. However, poor long term performance continues to limit the usefulness of this otherwise attractive material. The principal causes of thermoelement failures in the material include deterioration of the element to shoe bond and degradation of thermoelectric output because of composition changes within the element.

This program had, as its objective, the study of the bonding process and the determination of the mechanism or mechanisms of bond failure in lead telluride thermoelectric elements. A secondary objective was the development of a satisfactory braze and shoe system for the material. It was preferred, but not required, that the selected materials be nonmagnetic.

A systematic approach was applied to the selection and screening of potential braze and shoe materials for use with lead telluride. A literature survey reviewing work in bonding lead telluride at other installations was performed. This, plus analytical evaluation of available metallurgical data, led to the selection of a number of metals and alloys for use in the program. Although all materials of potential interest could not be studied, the group selected for evaluation is considered representative.

Preliminary screening was accomplished by carrying out wettability tests and accelerated poison effects tests. The first of these measured the ability of the braze materials to flow on and adhere to the surface of lead telluride and the various shoe materials. The poison effects test qualitatively studied the probable effects of long time diffusion of braze and shoe materials into lead telluride.

Tin telluride was found to be the braze having the smallest deleterious effect on the thermoelectric properties of lead telluride. Consequently, this compound was selected for study in bonded elements. A bonding process was developed and a number of elements were prepared and evaluated metallographically, by bond resistance measurements and by torque tests. A concurrent stress analysis task identified the principle thermal stress patterns present in bonded thermoelements and showed how they could be applied to the lead telluride bonding problem.

Several conclusions were drawn from this program:

(1) There are many shoe materials to which lead telluride may be bonded and an even larger number of brazes that will form a bond that is metallurgically sound initially.

(2) In most cases such bonded elements will not survive or perform adequately for extended periods of time under thermoelectric generator operating conditions.

(3) A principle cause of failure is poisoning by diffusion of material from the braze or shoe into the thermoelectric material. A poison may affect Seebeck coefficient, electrical resistance or both of these parameters. Test results showed that p-PbTe is more susceptible to degradation from this cause than is n-PbTe.

(4) Thermal stresses at the bond interface is the other major failure mechanism found during this study. The magnitude of the stress is related to the difference in thermal expansion between the element and shoe. This stress is partly relieved by deformation of the braze material. In the case of the TEG-2 lead telluride materials studied in this program the residual thermal stress is less than the fracture strength of the n-material but greater than the fracture strength of the p-material.

(5) SnTe or SnTe modified by titanium additions is a promising braze for joining PbTe to iron shoes. Life tests of properly designed and manufactured elements must be made to fully assess the utility of this system.

II. LITERATURE SURVEY

A survey of the technical literature was undertaken to study previous work in formation of element to shoe bonds in PbTe thermoelectric elements. Much of the earlier work was performed as part of module or generator programs and in these cases the objective was to find a satisfactory bond for a particular application. Two fairly detailed bonding studies were undertaken under Navy sponsorship by General Atomics (Reference 1) and Westinghouse (Reference 2).

At General Atomics (Reference 1) about fifteen alloys, mostly intermetallic compounds and eutectics, were tested as possible brazes for p- and n-type PbTe. Shoe materials were 0.005 inch thick sheets of iron, nickel, tin plated iron, tin plated nickel, and gold. Bonded specimens were checked for resistivity and were evaluated by life and cycling tests. Nickel shoes were generally superior to iron. A few couples bonded to gold shoes were unsatisfactory. Testing of bonded specimens had not been completed when the final report was prepared by General Atomics. Tentative conclusions were that several bond-shoe combinations were promising for use with n-type PbTe, including:

SnTe on Sn plated Fe

AuTe on Sn plated Ni

PbSe on Fe

InSb on 321 Stainless Steel

Four bonded p-type PbTe samples were tested and all showed drastic property changes within 100 hours. Better results were achieved with PbSnTe p-material.

Westinghouse (Reference 2) found that NiP or 302 stainless steel sprayed on 302 stainless foil made satisfactory bonds to n-type PbTe. Best results with p-PbTe were achieved by bonding the telluride with NiP to NiP coated gold foil. However, the expansion mismatch required that the gold deform, thereby limiting the thickness of foil. Earlier, as part of the Module Improvement Program, Westinghouse (Reference 3) had successfully tested two PbTe couples that were pressure bonded to iron hot straps and tin brazed to the cold shoe. The number of unsatisfactory modules were not reported.

All other reports obtained during this study in which PbTe bonding is discussed appeared to be based on limited work aimed at solving an immediate problem related to a larger program. Martin (Reference 4) and Tyco (Reference 5) independently developed bonding procedures based on a SnTe braze material. Very few test data were reported. General Electric (References 6 and 7) attempted to apply the Tyco process to a cartridge type element they were developing, but were not successful. Brazed joints separated after only a few thermal cycles.

General Electric (Reference 7) also tried hot pressed iron end caps and isostatically bonded iron caps on their PbTe elements. The first of these processes was unsuccessful while the isostatic pressing technique had not been fully evaluated at the time the project was completed.

Martin (Reference 4) has reported some success with nickel diffusion bonds at PbTe hot junctions and with tin brazing as a cold shoe joining method. Tin soldering of cold shoes has also been reported by General Instrument (Reference 8). Lead-tin solders are recommended for cold junctions by Minnesota Mining and Manufacturing (Reference 9).

Tyco (Reference 10) is performing a study under NASA sponsorship in which it is intended to develop bonds between PbTe and nonmagnetic shoe materials. Preliminary results indicate that SnTe brazing to tantalum shoes and diffusion bonding to tungsten shoes produce low resistance bonds. Life test data are not yet available.

As part of a generator development program DuPont (Reference 11) obtained satisfactory diffusion bonds between WSe_2 and p-type PbTe by heating under 150 psi to 500^{o}C in 40 percent air - 60 percent argon atmosphere.

None of the above studies has yet yielded the reliable long life element to shoe bonds required before PbTe thermoelectrics can be widely accepted for space missions.

III. MATERIALS AND EQUIPMENT

A. Materials

The thermoelectric and braze materials used in this program were high purity semiconductor quality products procured from commercial sources. The shoe materials were standard commercial grades. These are further described below.

1. Thermoelectric Material - PbTe

The lead telluride employed in this program was purchased from Minnesota Mining and Manufacturing Company in the form of powder. A few cold-pressed and sintered pellets were procured for comparison. The materials are identified as follows:

n-PbTe - Type TEG-2N

p-PbTe - Type TEG-2P

p-PbSnTe - Type TEG-3P

The purchased elements were made from TEG-2N and TEG-2P powders. In no case would 3M identify the dopants or exact composition of their lead telluride materials.

2. Braze Materials

Twelve elemental metals were purchased in the form of high purity powder, shot or lumps for use as brazes or in the preparation of braze alloys. Each was 99.999+ percent pure. All were procured from American Smelting and Refining Company, except for the tin which was purchased from Cominco Products, Incorporated. The elements purchased for this program and some of their properties are listed in Table 1.

3. Shoe Material

Samples of eleven shoe materials were procured in sheet form for preliminary bond evaluation. Those chosen for further study as a result of preliminary tests were also purchased in the form of one-half inch diameter bar stock. These alloys, significant properties and suppliers are listed in Table 2.

Table 1

Elemental Metals Purchased for Braze Alloy Preparation

Element	Melting Point, ^{o}C	Coefficient of Expansion $^{o}C^{-1} \times 10^{6}$
Antimony (Sb)	630.5	8 - 11
Bismuth (Bi)	271.3	13.3
Cadmium (Cd)	321	29.8
Copper (Cu)	1083	16.5
Gold (Au)	1063	14.2
Indium (In)	156.61	33
Lead (Pb)	327.4	29.3
Selenium (Se)	217	37
Silver (Ag)	960.5	19.7
Tellurium (Te)	990	16.75
Tin (Sn)	231.9	23.8
Zinc (Zn)	419.5	39.7

Table 2

Prospective Shoe Materials Procured for Testing

Alloy	Composition in Weight Percent	Melting Temp., ^{o}C	Coef. of Thermal Exp. $^{o}C^{-1} \times 10^{6}$	Supplier
Iron		1537	11.76	A. D. Mackay
Nickel		1453	13.3	A. D. Mackay
Columbium		2468	7.31	A. D. Mackay
Molybdenum		2610	4.9	A. D. Mackay
Beryllium		1277	11.6	A. D. Mackay
304 Stainless Steel	19 Cr, 10 Ni, 0.8 C, 2 Mn, 1 Si, Bal Fe	1400 - 1455	16.6	A. D. Mackay
Rene' 41	11 Co, 19 Cr, 10 Mo, 5 Fe, 1.5 Al, 3.2 Ti, 0.12 C, Bal Ni	1310 - 1345	13.5	Union Carbide
Haynes 25	10 Ni, 20 Cr, 15 W, 3 Fe, 1.5 Mn, 0.10C, Bal Co	1329 - 1410	12.3	Union Carbide
Multimet	20 Ni, 20 Co, 21 Cr, 3 Mo, 2.5 W, 1 Cb + Ta, 1 Si, 1.5 Mn, 0.12 C, Bal Fe	1288 - 1354	14.1	Union Carbide
Magnil	18 Cr, 15 Mn, 0.1 C, Bal Fe	----	17.9	American Silver Co.
Carpenter No. 10	18 Ni, 16 Cr, 0.08 C, Bal Fe	----	18.7	Carpenter Steel

B. Equipment

Three items of special equipment were designed and manufactured for this program. These were used for measurement of room temperature electrical resistivity, Seebeck coefficient, and torque strength of bonded elements. These devices are shown schematically in Figures 1 through 3. All resistivity and Seebeck measurements were made with a Honeywell Model 2733 precision potentiometer which could be read to 1 microvolt in the 0 - 11 millivolt range and 10 microvolts in the 11 - 110 millivolt range.

All other operations were performed with standard laboratory equipment, some of which was modified specifically for this program. For example, hot pressing of thermoelectric elements was performed in an inert atmosphere plexiglas chamber. Power was supplied by a 12.5 KVA Lepel induction unit and load applied with a Carver Laboratory Press.

Wettability tests were carried out in a Lindberg tube furnace equipped with inconel muffle and purified argon atmosphere. The tank argon was deoxidized by passing over heated calcium chips and dried by successively passing through two dry ice - acetone cold traps and a Drierite unit. This equipment is shown in Figure 4.

Bonding was performed in the stainless steel and graphite fixture shown in Figure 5. This was inserted in a vycor tube closed at one end. Fittings at the other end permitted evacuation of the entire setup and subsequent back-filling with argon. Heating was accomplished by inserting the vycor tube into a furnace.

Other equipment employed included conventional furnaces, balances, and vacuum systems, etc.

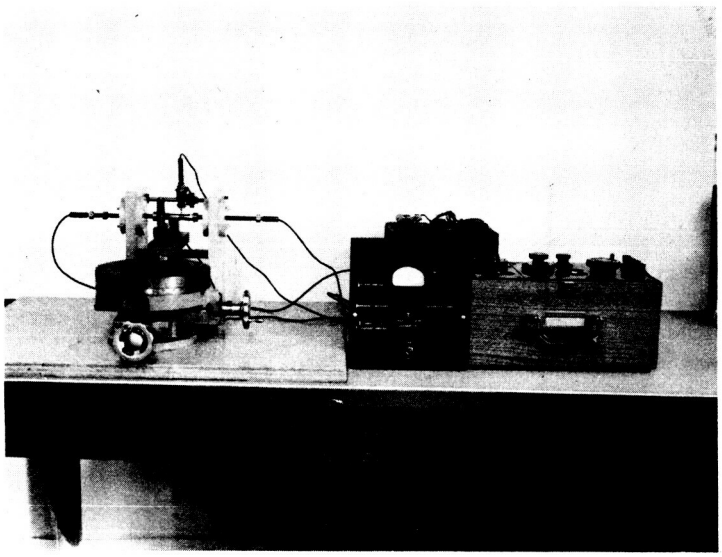

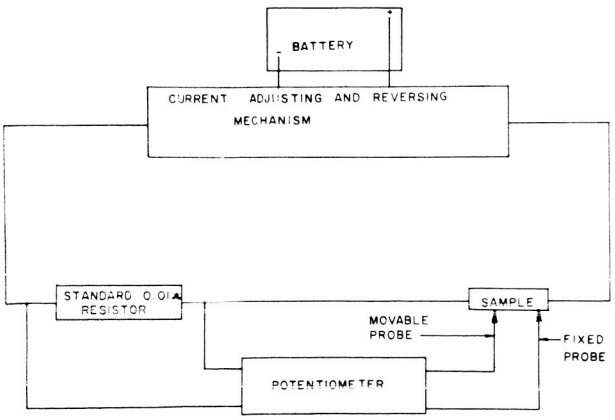

Figure 1. Resistivity Test Apparatus

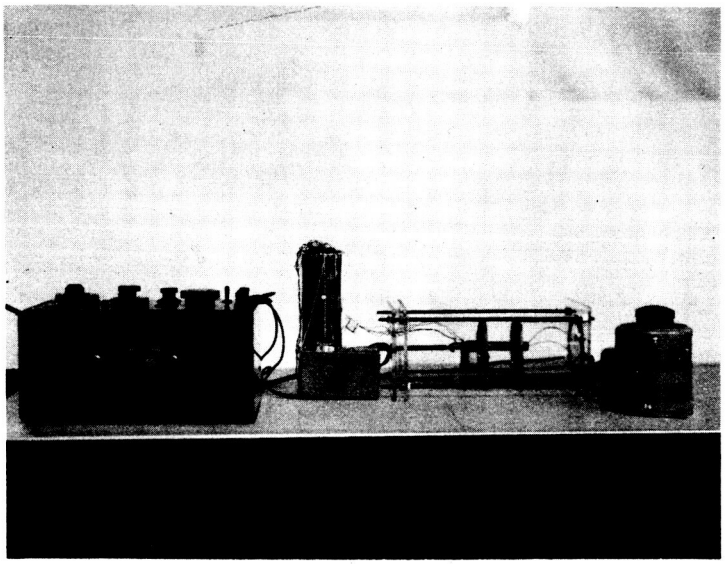

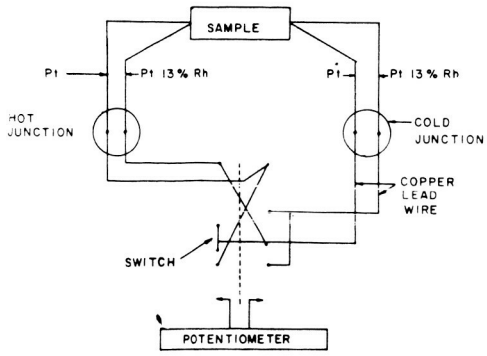

Figure 2. Seebeck Test Apparatus

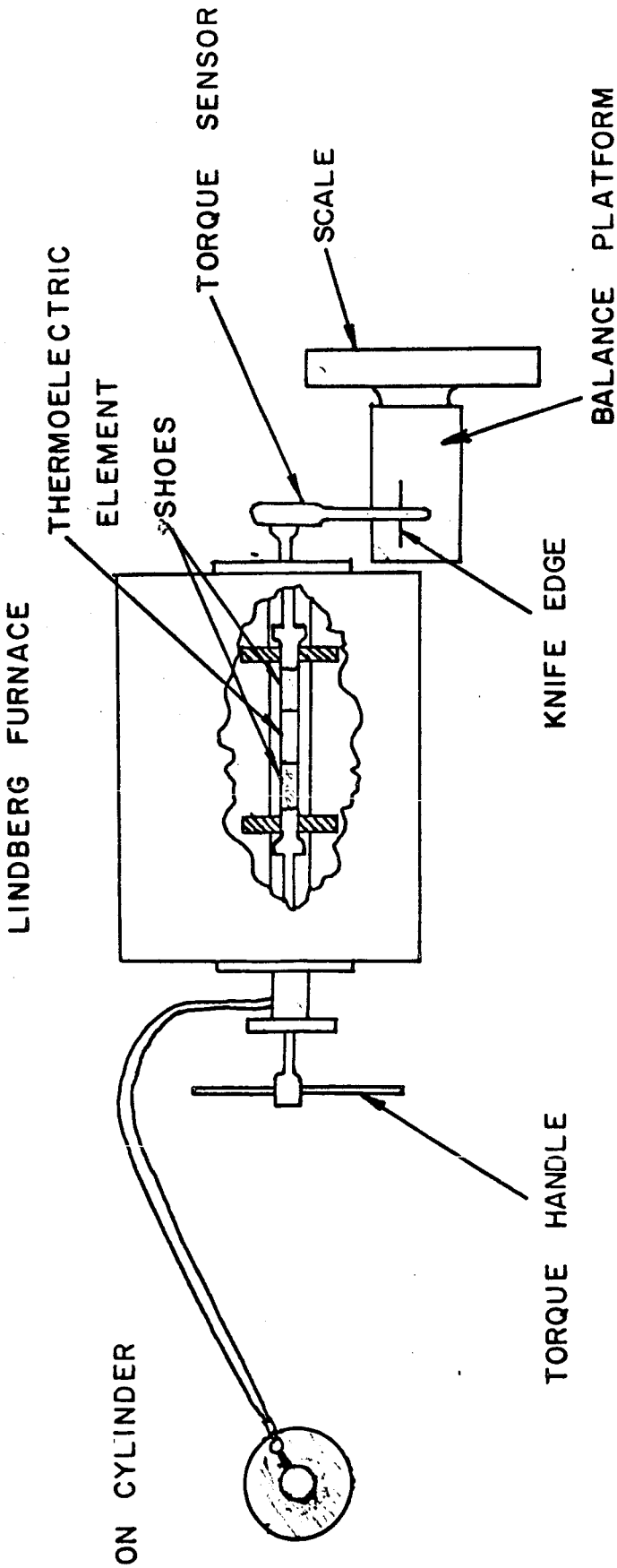

FIGURE 3. PLAN VIEW OF TORSION TEST SETUP

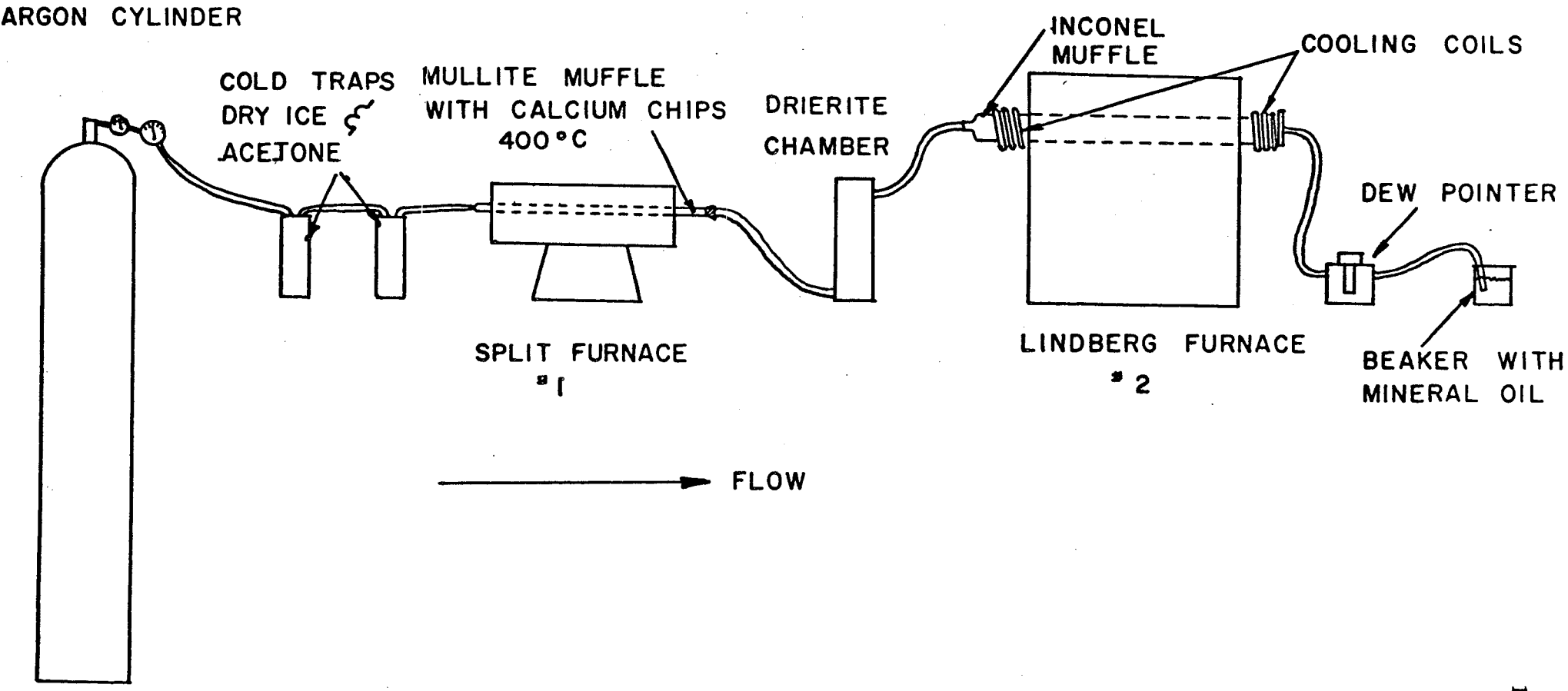

FIGURE 4. SCHEMATIC OF WETTABILITY TEST SETUP

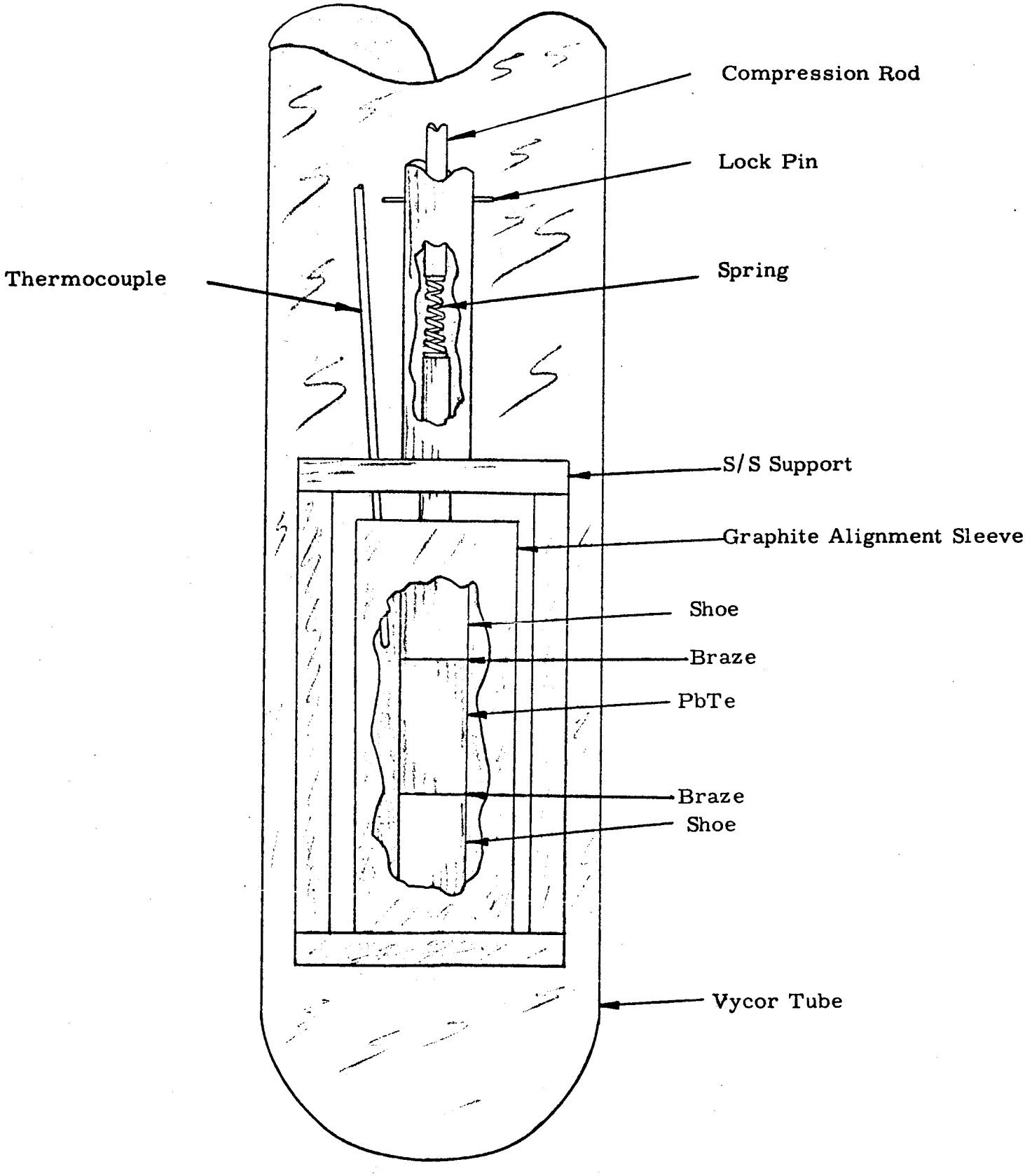

FIGURE 5. THERMOELECTRIC BONDING APPARATUS

IV. PRELIMINARY BRAZE AND SHOE MATERIAL EVALUATION

The first phase of the laboratory program was concerned with the selection of several braze alloys, preliminary evaluation of these alloys, and the decision to continue work on several of these brazes. A preliminary evaluation of shoe materials was similarly performed.

This preliminary evaluation consisted of wettability tests in which the flow and adhesion of each selected braze on p-PbTe and n-PbTe was determined. Those brazes which gave some positive indication of wetting on PbTe were tested on each of the potential shoe materials.

The following paragraphs describe the preparation of the PbTe thermoelectric elements employed in these and subsequent tests, the braze and shoe materials selected, and the procedures and results of the wettability tests.

A. Preparation of Lead Telluride Elements

Almost all the thermoelectric elements used in the course of this program were fabricated from powders in our laboratory. The need to incorporate additives in the elements for the poison effects study and the general desirability of having elements made by a consistent process were the reasons for our decision to fabricate in-house.

Lead telluride elements were manufactured by a hot-pressing technique. This process is described as follows. The correct amount of powder was weighed out. If a poison additive was included the weighed powders were placed in a glass bottle and tumble mixed for one hour. The PbTe or blended powder was then loaded into a single action graphite die. Faces of the top and bottom punches were coated with high purity alumina to insure easy removal of the pressed pellet. New dies were baked out at or near the hot pressing temperature prior to use to eliminate volatiles that might contaminate the product.

The die was placed into an inert atmosphere chamber which consisted of a nine inch cube of plexiglas. Lead throughs were available for an induction coil, argon inlet and outlet, and a piston through which the load was applied. The chamber was then purged with argon, heat was applied through the 12.5 Kw induction unit. The die was raised to temperature and the load was applied and held for the requisite amount of time.

Two sizes of PbTe elements were produced, 3/8 inch diameter by 5/8 inch high, and 1/2 inch diameter by 3/4 inch high. The smaller elements were manufactured for wettability tests only. All other tests and measurements were made on one-half inch diameter elements. Several hundred p- and n-PbTe pellets were hot pressed during this program. The manufacturing parameters are described in Table 3. Hot pressing time was 15 minutes during early runs and was reduced to about 5 minutes later in the program with no measurable change in density or properties.

Table 3

Hot Pressing Conditions for PbTe Thermoelectric Elements

Material	Type	Diameter, Inches	Load, tsi	Temperature, °C	Time at Pressure, Minutes
TEG-2N	n-PbTe	3/8	1.25	744	15
TEG-2P	p-PbTe	3/8	1.25	760	15
TEG-2N	n-PbTe	1/2	1.25	788	5 - 15
TEG-2P	p-PbTe	1/2	1.25	760	5 - 15
TEG-3P*	p-PbSnTe	1/2	1.25	760	5

* Not optimum

A few, 1/2 inch diameter TEGS-3P, p-PbSnTe elements were also hot pressed during the latter part of this program. No attempt was made to optimize pressing conditions for this material. The hot pressing parameters employed in the manufacture of these pellets are also listed in Table 3.

Hot pressed PbTe pellets appeared to be sound. Densities were in excess of 97 percent of theoretical. Metallographic examination indicated virtually no porosity compared with extensive porosity in 3M cold-pressed and sintered elements. The p-PbSnTe pellets did not achieve as high a density. No 3M produced p-PbSnTe elements were available for comparison.

The PbTe elements produced in our laboratory displayed thermoelectric properties quite comparable to those reported by 3M. Electrical resistivity values for several Hittman produced p- and n-type PbTe elements are shown in Table 4 and are compared herein with measurements made in our laboratory on 3M produced elements and with electrical resistivity values given in 3M technical literature. These data for n-PbTe generally fall within the $\pm$ 10 percent variation in resistivity claimed by 3M for their own products and are consistently lower than the 3M average. The p-PbTe resistivities averaged about 15 percent below the 3M values.

Figure 6 shows the values of Seebeck coefficient measured on p- and n-PbTe elements produced at Hittman Associates and compares them to the values reported by 3M. The dashed lines define the 10 percent deviation limits. It can be seen that the Hittman produced n-type elements fall uniformly within these limits, while the p-type PbTe generally fall in the 3M limits with some deviation on the high side.

B. Selection and Preparation of Braze Alloys

Prospective braze alloys were selected on the basis of the following criteria:

(1) Melting point below that of PbTe (917^{o}C).

(2) Expectation that serious poisoning would not occur.

(3) Expected remelt temperature above device operating temperature.

Other desirable criteria such as wettability and compatible coefficient of thermal expansion could not be applied because of a lack of reliable data. On the above basis the materials listed in Table 5 were selected for preliminary evaluation as braze materials. Those containing copper and silver, known poisons to PbTe, were selected for use as controls to check our instrumentation.

Table 4

Room Temperature Electrical Resistivity
of PbTe Elements Hot Pressed at Hittman Associates

(a) p-PbTe

Source	Resistivity, microohm-inches	
Hittman Associates	139	
Hittman Associates	124	
Hittman Associates	148	
Hittman Associates	135	140 average
Hittman Associates	157	
Hittman Associates	135	
3M TEGS-2P -- Tested at Hittman Associates	188	
3M Literature -TEGS-2P	165	

(b) n-PbTe

Hittman Associates	166	
Hittman Associates	181	
Hittman Associates	195	182 average
Hittman Associates	181	
Hittman Associates	185	
3M TEGS-2N -- Tested at Hittman Associates	202	
3M Literature - TEGS-2N	200	

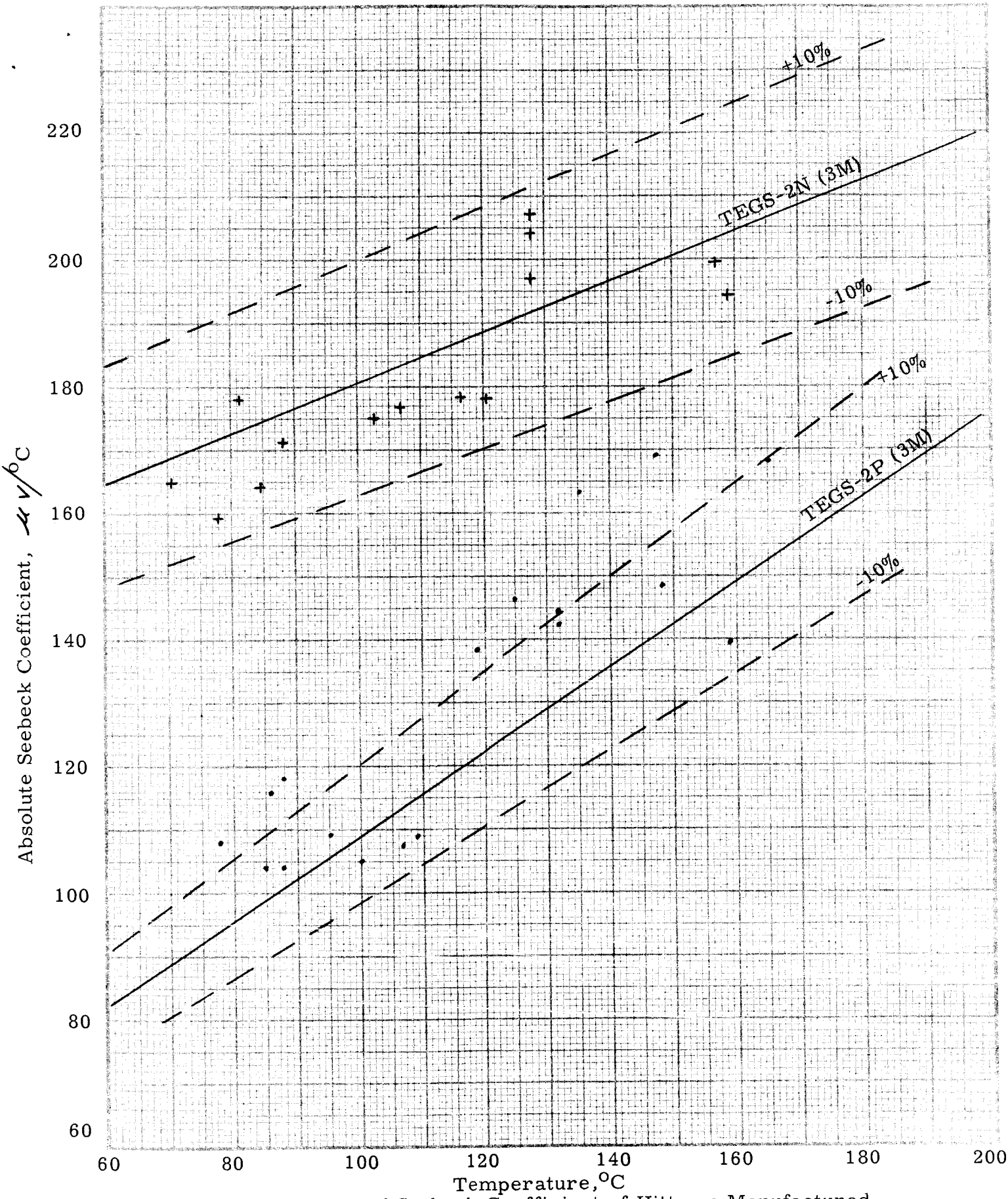

Figure 6. Comparison of Seebeck Coefficient of Hittman Manufactured PbTe With 3M Literature Values

Table 5

Potential Braze Alloys Selected for This Study

Alloy	Type of Alloy	Melting Point, °C
SnTe	Compound	790
Bi_2Te_3	Compound	585
InSb	Compound	530
CdSb	Compound	456
InSe	Compound	660
InTe	Compound	696
Sb_2Te_3	Compound	622
AuZn	Compound	725
56% Ag - 44% Sb	Eutectic	485
51% In - 59% Au	Eutectic between AuIn and $AuIn_2$	494
76.5% Sb - 23.5% Cu	Eutectic	526
79.9% Sb - 20.1% Zn	Eutectic	505
70% Sb - 30% Bi	Solid Solution	430
Sn	Elemental	232
Bi	Elemental	271
Se	Elemental	217
Sb	Elemental	631
In	Elemental	157
Cu	Elemental	1083

Braze alloys were prepared by the following procedure. The components of the alloy or compound were carefully weighed out to the nearest milligram and were placed in a vycor or pyrex glass capsule. The capsule was pumped down by a mechanical vacuum pump, backfilled with argon and then pumped down again. A minimum of ten pumping, filling cycles were employed. Following the last pumpdown the capsule was sealed. Each alloy was taken above its melting temperature, removed from the furnace, agitated and reheated at least five times. The capsule was then air cooled to room temperature. Metallographic and visual examination showed that all the alloys were homogeneous and sound except for InSe which could not be successfully prepared in two trials. No further work was performed with this material.

C. Selection of Shoe Materials

Samples of eleven prospective shoe materials were procured in sheet form for wettability tests with selected braze alloys. The shoe materials were selected so as to cover as many classes of material as possible. Columbium and molybdenum, for example, are refractory metals, beryllium is a light metal, iron, nickel, and 304 stainless represent the conventional engineering materials, and Haynes 25, Rene' 41 and Multimet are examples of nickel and iron base superalloys. Both nonmagnetic and magnetic alloys were included. The entire list of shoe materials was given previously in Table 2.

D. Wettability Tests

A preliminary evaluation of braze and shoe materials was performed by checking the wettability of each of the braze materials on PbTe. Those that appeared promising were tested on each of the potential shoe materials. The wettability of each of the shoe materials by PbTe was also checked. The tests were carried out in the Lindberg furnace setup pictured schematically in Figure 4 above. The argon atmosphere was maintained at a dewpoint of $-50^{\circ}C$ or better.

Tests of the wettability of PbTe by various braze materials were carried out in the following manner. For each test wafers of n-PbTe and p-PbTe were placed on an alumina plate. A sample of the braze to be evaluated was placed on top of each wafer and the assembly was carefully inserted into the furnace. The muffle was purged for at least one hour and the sample was then heated until signs of melting of the braze were visually observed through a plexiglas port.

The samples were examined visually and were then cut through the bond with a jeweler's saw and mounted for metallographic examination. Table 6. shows the results of these tests and identifies those braze materials chosen for further study.

Table 6

Wettability of PbTe by Braze Materials

Braze Material	Braze Melting Temp. °C	Max. Test Temp. °C	Results	Chosen for Continued Evaluation
Sn	273	270	poor flow but good adherence	X
Bi	271	300	good flow and adherence	X
Se	217	233	good flow and adherence	
Sb	631	700	poor flow, good wetting	
In	157	192	poor flow, no bond	
Cu	1083	657	entire sample had melted, the 500°C Cu-PbTe eutectic temperature was exceeded	
SnTe	790	860	good flow, excellent wetting, some cracks and pores, retest showed no pores	X
Bi_2Te_3	585	648	excellent flow and wetting, pores in Bi_2Te_3 adjacent to interface	X
InSb	535	525	good flow and wetting, cracks in PbTe	X
CdSb	456	612	braze separated from n-PbTe before mounting; p-PbTe sample had two intermediate phases and poor flow	
InTe	696	747	excellent flow and wetting, some pores and cracks in InTe	X
Sb_2Te_3	622	670	Good to excellent flow and wetting, pores in p-PbTe adjacent to interface, signs of cracking or separation in n-PbTe interface	X
AuZn	725	869	no bond formed	

Table 6 (Cont.)

Braze Material	Braze Melting Temp. °C	Max. Test Temp. °C	Results	Chosen for Continued Evaluation
56% Ag - 44% Sb	485	666	extensive penetration into PbTe, good flow, phase in interface	X
41% In - 59% Au	494	582	poor flow, poor bond	
76.5% Sb - 23.5% Cu	526	673	good flow and wetting	
79.9% Sb - 20.1% Zn	505	649	poor flow, two phases in interface	
70% Sb - 30% Bi	430	665	good flow and wetting, few cracks in PbTe	X

Choice was made on the basis of test results. However, program limitations made it necessary to remove from further consideration some materials that were of marginal interest. At least one material was chosen from each group, elements, intermetallic compounds, eutectics and solid solutions.

Wettability tests on shoe materials were carried out in a similar manner. In this case sheet samples of nine of the shoe materials (Magnil and Carpenter No. 10 were obtained later and tested separately) were placed on the alumina plate and the braze to be evaluated was placed on each. Test and evaluation procedures were identical with those described above. The results of these tests are reported in Table 7. Results of wetting tests of PbTe on each shoe material are included in this table.

In no case was a flux used to aid wetting. Sample preparation consisted of abrasion to remove surface oxides followed by degreasing in acetone. The reported results are indicative but are not conclusive evidence of the bonding that may be obtained by varying the cycle parameters. It is clear that bonding will be more readily attained with the iron, nickel and cobalt base alloys than with beryllium or the refractory metals.

Shoe \ Braze	InSb	SnTe	Bi_2Te_3
Beryllium	No flow; bond broke with light pressure	No flow; poor bond	Fair flow; poor bond
Columbium	Poor flow and bond	No flow; poor bond	Fair flow; poor bond
Iron	Good flow, no tarnish; broke while sawing	Good flow; bond broke while sawing; reaction zone	Good flow; poor bond; broke while sawing
Molybdenum	Poor flow; bond looked good but broke while sawing	Good flow; bond broke while sawing	Fair flow; no bond
Nickel	Excellent flow and bond; slight reaction zone	Excellent flow; poor bond	Excellent flow; poor bond
Haynes - 25	Poor flow and bond	Excellent flow; good bond; reaction zone	Excellent flow; metallography shows poor bond
Multimet	Poor flow and bond	Very good flow; reaction zone; bond separated	Excellent flow; good bond; reaction zone
Rene' 41	Poor flow and bond	Good flow; poor bond; reaction zone	Good flow; poor surface appearance
304 Stainless	Poor flow and bond	Good flow and bond	Excellent flow; good bond
Magnil (0.003")	----------	Good flow and bond	Good flow; no bond
Carpenter No. 10	Poor flow; no bond	Good flow and bond	Good flow and bond; diffusion zone

Table 7

of Wettability Test Results of Brazes on Shoe Materials

InTe	Sb_2Te_3	56 w/o Ag - 44 w/o Sb	70 w/o Sb - 30 w/o Bi
No flow or bond	No flow or bond	No flow or bond	No flow or bond
Poor flow; no bond	Poor flow and bond	No flow or bond	No flow or bond
Poor flow; no bond	Excellent flow; metallography indicates bond poor	No flow or bond	No flow or bond
Poor flow; no bond	Poor flow; no bond	No flow or bond	No flow or bond
Complete reaction; no sign of nickel	Poor flow; good bond	No flow or bond	Poor flow and bond
Good flow; bond intermittent but good where present	Excellent flow; good bond	No flow or bond	No flow; poor bond
Good flow and bond; cracks in InTe away from bond	Excellent flow; metallography shows bond separation	No flow or bond	No flow or bond
Good flow; poor bond	Very good flow; some bond separation	No flow or bond	No flow; poor bond
Good flow and bond	Excellent flow; reaction zone; Sb_2Te_3 cracked	No flow or bond	No flow or bond
Poor flow and bond	Bad reaction	----------	----------
Good flow and bond; InTe cracked	Good flow; cracks in interface	----------	Good flow and bond

Sn	Bi	PbTe
No flow or bond	Poor flow; no bond	Fair flow; PbTe cracked; bond poor
No flow or bond	No flow or bond	Good flow; poor bond
Poor flow; good bond	No flow or bond	Good flow; poor bond
No flow or bond	No flow or bond	Good flow; reaction zone; bond separation
Good flow and bond; reaction zone	Fair flow; good bond	Fair flow; reaction zone; porosity in PbTe
No flow or bond	No flow or bond	Good flow; reaction zone; bond separation
No flow or bond	No flow or bond	Good flow and bond; reaction zone
No flow or bond	No flow or bond	Very good flow; cracking in PbTe phase
No flow or bond	No flow or bond	Good flow; poor bond
No flow or bond	----------	----------
No flow or bond	Poor flow; no bond	----------

V. POISONING EFFECTS STUDY

Preparation of suitable element to shoe bonds in PbTe thermoelectric elements requires the satisfaction of two principal criteria. First, the bond must be mechanically sound initially and must remain sound throughout the required lifetime. Second, the diffusion of material from the shoe and/or braze into the thermoelement must not deleteriously affect the thermoelectric properties of the material. The sturdiest bond will be unsatisfactory if the thermoelectric output declines as a result of diffusion from the bond into the elements.

Therefore, as a further screening tool, tests were undertaken to determine the effect of small additions of prospective braze and shoe materials on the thermoelectric properties of PbTe. Two series of experiments were performed, one in which only the as hot-pressed properties were measured and a second in which the effect of time at 538°C (1000°F) was also considered. These experiments were in the nature of accelerated tests. In each case the prescribed amount of foreign additive was dispersed in the PbTe powder prior to hot pressing in order to simulate a condition analogous to one that might result from diffusion mechanisms after hundreds or thousands of hours of operation at elevated temperatures.

The first test series was performed as follows. One n-PbTe and one p-PbTe sample containing each contaminant was prepared by the standard hot pressing technique for one-half inch diameter samples described in Chapter IV. Generally one percent by weight of the additive was employed, the only exceptions being in the case of nickel where a few samples containing smaller amounts were prepared. In several cases duplicate samples were run and good qualitative agreement was obtained.

Eighteen additives were employed in this study:

SnTe	70 w/o Sb - 30 w/o Bi	Fe
Bi_2Te_3	SnTe - 1 w/o Ti	Mo
InTe	SnTe - 1 w/o V	Cb
Sb_2Te_3	Sn	347 SS
InSb	Bi	Carpenter No. 10
56 w/o Ag - 44 w/o Sb	Cu	Ni

Generally, the specimens containing additives to the easily hot pressed n-PbTe could be fabricated about as well as the unpoisoned samples. P-PbTe, which is more difficult to fabricate, presented some problems when samples containing some of the braze materials were required. Several pressings were frequently required to obtain a sound element. On the other hand certain additives, notably molybdenum and columbium, resulted in p-PbTe elements that were excellent in appearance and that appeared substantially stronger than the ordinary p-type material. Although development of improved lead telluride materials was not within the scope of the work, the above observations may warrant further investigations.

Resistivity and Seebeck coefficient measurements were made on each sample using the equipment described previously. The results are given in Table 8. In this table are listed the Seebeck and electrical resistivity measurements made on each sample plus the calculated deviation from mean values for unpoisoned p- and n-PbTe.

It is obvious from these results that SnTe and the two modified SnTe materials have substantially less deleterious effect on PbTe than any of the other brazes studied. For these alloys an increase in the resistivity of p-PbTe of 40 - 140 percent with 1 w/o SnTe is the largest degradation observed. The additions of Ti and V to the SnTe braze reported in Table 8 were made primarily to improve bond strength as discussed in Chapter VI. However, it can be noted that the braze with these additions also shows less degradation of resistivity in p-legs than straight SnTe. Of the shoe materials the observed effects were inversely proportional to the melting temperature of the additive. That is, the smallest property changes occurred with molybdenum and columbium additives, greater changes were observed with iron, nickel, and stainless steel, and the most drastic effects occurred when copper was added.

In all cases the effects were significantly greater in p-PbTe than in n-PbTe. This is in general agreement with other studies of PbTe.

One sample of p-PbTe to which was added 1/10 w/o Ni showed no poisoning effect, indicating that the threshhold is between 1/10 and 1 weight percent for that additive.

Subsequent to the electrical property measurements each pellet was cut and mounted so that metallographic examination could be performed of transverse and longitudinal sections. All of the potential shoe materials could be seen present as discrete second phases uniformly dispersed in a lead telluride matrix. This was generally true of the braze additives also. Lead tellurides containing tin telluride appeared to be largely single phase and in the case of the Bi_2Te_3, InSb and Sn there were signs of at least partial solution into the lead telluride matrix.

The above observations led to the probability that further poisoning effects might be observed if PbTe containing additives were held at elevated temperatures in order to allow further solutioning of the additive. For this reason several samples containing one percent additions of SnTe, SnTe - 1 w/o Ti, Sn, Fe, and Carpenter No. 10 alloy were prepared and tested at 538°C (1000°F) for times up to 600 hours. Several unpoisoned control samples were tested at the same time.

The test procedure was as follows. The Seebeck coefficient and electrical resistivity of each sample was measured after hot pressing. Each sample was then placed in an individual vycor capsule which was evacuated and backfilled with argon several times and then sealed under one-half atmosphere of argon. The sealed vycor capsules were then placed in a furnace, heated to the test temperature and held for the desired length of time. Samples were removed and properties remeasured after intervals of about 100, 300, 400 and 600 hours. After one or two cycles all the p-PbTe materials

Table 8

The Effect of Poison Additives on the Seebeck Coefficient and Resistivity of PbTe

Material	Sample No.	Seebeck Coefficient Data: Temp. °C	S, μV/°C	% Deviation From PbTe*	Electrical Resistivity: ρ, μΩ-in.	% Deviation From PbTe
n-PbTe + 1 w/o SnTe	51	108	-175	-5	172	-5
		163	-199	-3		
	178	94	-173	-3	176	-3
		140	-204	+4		
p-PbTe + 1 w/o SnTe	53	105	+122	+8	343	+145
		159	+162	+9		
	179	93	+102	-2	218	+56
		152	+162	+12		
n-PbTe + 1 w/o Bi_2Te_3	48	106	-58	-68	123	-32
		163	-76	-63		
p-PbTe + 1 w/o Bi_2Te_3	47	104	-51	-100 p to n	2570	+1700
		158	-63	-100		
n-PbTe + 1 w/o InTe	46	104	-211	+16	799	+340
		159	-249	+22		
p-PbTe + 1 w/o InTe	45	110	+149	+28	10000	+7000
		168	+187	+21		
n-PbTe + 1 w/o Sb_2Te_3	35	105	65	uncertain whether	94	-48
		175	82	p or n		
p-PbTe + 1 w/o Sb_2Te_3	39	91	+226(?)	+119(?)	666	+376
		146	+197	+41		
	75	95	+158	+49	851	+597
		147	+192	+37		
n-PbTe + 1 w/o InSb	54	103	-210	+15	785	+331
		159	-228	+12		
p-PbTe + 1 w/o InSb	55	92	+252	+142	6280	+4400
		138	+406	+202		

Table 8 (Cont.)

Material	Sample No.	Seebeck Coefficient Data: Temp. °C	S, μV/°C	% Deviation From PbTe*	Electrical Resistivity: ρ, μΩ-in.	% Deviation From PbTe
n-PbTe + 1 w/o Ag-Sb	38	101	-363	+101	8600	+4600
		159	-383	+88		
p-PbTe + 1 w/o Ag-Sb	84	78	+57	-40	8780	+6100
		118	+173	+43		
n-PbTe + 1 w/o Sb-Bi	56	113	-93	-50	104	-43
		173	-115	-45		
p-PbTe + 1 w/o Sb-Bi	57	109	-95	-100 p to n	134	-4
		165	-113	-100		
n-PbTe + 1 w/o (SnTe - 1 w/o Ti)	243	86	-179	+2	213	+17
		126	-198	+4		
p-PbTe + 1 w/o (SnTe - 1 w/o Ti)	242	83	+113	+15	220	+57
		130	+158	+22		
n-PbTe + 1 w/o (SnTe - 1 w/o V)	268	94	-152	-15	187	+3
		133	-170	-12		
p-PbTe + 1 w/o (SnTe - 1 w/o V)	267	84	+106	+8	194	+39
		125	+135	+7		
n-PbTe + 1 w/o Sn	59	103	-184	+1	209	+15
		157	-212	+4		
p-PbTe + 1 w/o Sn	60	96	+166	+56	2110	+1400
		154	+213	+47		
	85	95	+123	+16	2290	+1500
		143	+174	+26		
n-PbTe + 1 w/o Bi	62	101	-65	-64	87	-52
		167	-86	-58		

Table 8 (Cont.)

Material	Sample No.	Seebeck Coefficient Data: Temp. °C	S, μV/°C	% Deviation From PbTe*	Electrical Resistivity: ρ, μΩ-in.	% Deviation From PbTe
p-PbTe + 1 w/o Bi	63	104	-56	-100 p to n	353	+152
		163	-68	-100		
n-PbTe + 1 w/o Cu	64	106	-80	-56	87	-52
		164	-104	-50		
p-PbTe + 1 w/o Cu	67	104	-190	-100 p to n	369	+164
		154	-224	-100		
n-PbTe + 1 w/o Fe	73	97	-190	+6	172	-5
		158	-217	+7		
p-PbTe + 1 w/o Fe	70	99	+211	+94	475	+239
		152	+249	+73		
	172	96	+179	+68	506	+261
		149	+229	+61		
n-PbTe + 1 w/o Mo	81	97	-166	-8	150	-18
		150	-188	-6		
p-PbTe + 1 w/o Mo	82	96	+88	-17	156	+11
		153	+127	-12		
	280	91	+80	-22	139	-1
		129	+110	-14		
n-PbTe + 1 w/o Cb	86	95	-162	-9	177	-3
		145	-172	-13		
p-PbTe + 1 w/o Cb	88	99	+108	0	189	+35
		153	+141	-2		
n-PbTe + 1 w/o 347 SS	74	94	-177	-1	177	-3
		144	-200	+1		
p-PbTe + 1 w/o 347 SS	76	92	+178	+72	520	+271
		143	+213	+55		

Table 8 (Cont.)

Material	Sample No.	Seebeck Coefficient Data: Temp. °C	S, μV/°C	% Deviation From PbTe*	Electrical Resistivity: ρ, μΩ-in.	% Deviation From PbTe
n-PbTe + 1 w/o Carpenter No. 10	177	105	-172	-6	163	-10
		152	-190	-6		
n-PbTe + 1/2 w/o Ni	270	89	-157	-11	176	-3
		133	-206	+6		
n-PbTe + 1 w/o Ni	78	96	-183	+2	194	+7
		149	-203	+2		
p-PbTe + 1/10 w/o Ni	269	88	+112	+11	149	+6
		116	+145	+21		
p-PbTe + 1 w/o Ni	69	108	+175	+53	7075	+5000
		158	+220	+49		
	83	92	+145	+39	8860	+6200
		142	+188	+37		
	174	100	+155	+42	7670	+5400
		149	+211	+49		
	194	99	+141	+30	7640	+5400
		149	+189	+33		

Seebeck values for PbTe are those reported by 3M.

Resistivity values for PbTe are average of Hittman produced materials $\rho_n = 182\ \mu\Omega$-in.
$\rho_p = 140\ \mu\Omega$-in.

* Sign convention for Seebeck deviation is such that + deviation is beneficial for p and n material.

with and without additives were found to have high electrical resistivity. Several broke during test and the others had visible cracks present. Therefore, no useful data were obtained.

The data obtained on hot pressed n-PbTe and n-PbTe containing several additives are reported in Table 9. Measurements performed on unpoisoned lead telluride indicate its properties to be within the normally expected ten percent variation. Samples containing additions of tin and iron indicate some degradation after 600 hours at temperature. The results for SnTe indicate little change over the 600 hour test period. Similar results are seen for SnTe - Ti additive after the 113 hour test.

These limited results support the selection of SnTe and modified SnTe as superior braze alloys for lead telluride. They also point up the need for improved p-type lead telluride materials.

As a result of the need for better p-type material, a supply of TEG-3P PbSnTe powder was obtained from 3M Company. A few additive test samples were prepared from this material, but because of the non-optimum fabrication conditions employed, the results were ambiguous. Further study in this area is needed.

Table 9

Effect of Aging at 538°C on the Thermoelectric Properties of n-PbTe Containing Additives

Material	Sample No.	Time at 538°C Hours	Percent Deviation From Average PbTe Values Seebeck	Resistivity
n-PbTe	185	0	+3	-9
		96	-3	-2
		322	-7	+4
n-PbTe	190	0	+1	-1
		96	0	+7
		322	0	+7
n-PbTe + 1 w/o SnTe	196	0	-12	+4
		111	-6	+33(?)
		443	-15	+5
		599	-8	+7
n-PbTe + 1 w/o Sn	175	0	-6	-3
		111	-4	+1
		443	-16	-8
		599	-17	+7
n-PbTe + 1 w/o (SnTe-Ti)	243	0	+2	+17
		113	-2	+12
n-PbTe + 1 w/o Fe	173	0	+2	-5
		111	-2	+2
		443	-19	-10
		599	-9	-13

VI. BOND PREPARATION AND EVALUATION

The results of the screening tests described in the preceeding chapters were applied to the selection of braze and shoe systems for evaluation in the form of bonded thermoelectric elements. Tin telluride was the braze chosen for detailed evaluation. When some difficulties were encountered in producing reliable bonds, the titanium and vanadium additions to the braze material were developed.

The shoe material chosen for detailed evaluation was iron. Some bonds were made with nickel, Multimet and Haynes-25 shoes, but time limitations prevented extensive study of these metals. Carpenter No. 10 alloy was also selected for study, but could not be obtained in the form of suitable bar stock.

Bond specimens in all cases consisted of one-half inch diameter elements and shoes. Element length was 5/8 to 3/4 inch. Shoe length in most bonded elements was one inch. This length was selected for convenience in torque testing the thermoelectric elements. A few bonds were made with 1/8 to 1/4 inch shoes, primarily for convenience in mounting for metallographic examination.

A. Bond Preparation

A few early bonding experiments were performed by placing the shoes, braze and thermoelements into a graphite hot pressing die and applying about one tsi pressure at 790°C. SnTe braze, in the form of powder, was employed. The results were generally unsatisfactory. Subsequently, all bonds were made in the fixture pictured in Figure 5 (Chapter III). Preliminary bond runs were made with the SnTe braze in the form of powder, cold pressed disks and cold pressed disks sintered in hydrogen or argon atmosphere. The most consistent satisfactory results were obtained when pressed and sintered braze disks were used. Little difference resulted from the choice of atmosphere

The standard procedure employed in the preparation of braze wafers was as follows. Melted SnTe was ground to powder. The fresh powder was pressed into wafers of 1/4 or 3/8 inch diameter by approximately 0.010 inch thick. The wafers, separated by alumina sand, were placed into a vycor capsule which was evacuated and backfilled with argon several times and finally sealed under one-half atmosphere of argon. The sealed capsule was placed in a furnace and held at 600°C for about one hour. The sintered wafers were then placed in methanol for storage until used.

Similarly, several techniques for the preparation of the mating surfaces on the shoe and element were investigated. Three conclusions quickly emerged from these experiments. For the attainment of sound bonds:

(1) It is necessary to maintain the mating surfaces parallel to one another.

(2) Absolute cleanliness is required.

(3) Proper surface preparation is required.

The optimum element and shoe preparation methods developed during this program were as follows:

(1) Shoes: This procedure was followed for iron, nickel and alloy shoes.

The machined shoe was polished successively on 240, 320, 400, and 600 grit paper and then finished on polishing wheels with No. 3 universal diamond paste followed by 1 micron alumina. The shoe was then scrubbed in hot soapy water, rinsed in clear water, wiped with acetone, rinsed with methanol and stored in methanol until used.

(2) p-PbTe:

Hot pressed p-type elements normally had small chips missing at the corners. The elements were ground flat on 180 grit paper until a complete circular cross section was achieved. Almost 1/16 inch was usually removed from each end. Following this operation the procedure was identical to that used with the shoe materials.

(3) n-PbTe:

About 1/32 inch was ground from each end of the elements. Parallel score marks were then made by drawing the elements in one direction across 180 grit paper. The elements were then cleaned in soapy water, rinsed with water, wiped with acetone, rinsed with methanol and stored in methanol.

Elements were bonded in the following manner. The shoes, element and braze wafers were removed from the methanol in which they were stored and dried with clean Kimwipes. Differences in flow characteristics required use of 1/4 inch diameter wafers with p-PbTe and 3/8 inch diameter wafers with n-PbTe. The components were assembled and placed in a graphite alignment sleeve which was in turn inserted into the steel brazing jig (See Figure 5, Chapter III). Light pressure was applied through a spring to hold the assembly in position. The assembly was inserted into a large vycor tube which was sealed, evacuated and purged with argon. A small argon flow was maintained. The vycor tube was inserted into a furnace. The temperature was raised to 790° - 800°C, held for five minutes and allowed to furnace cool to about 600°C.

The assembly was then placed into a brick holding chamber which allowed it to slowly cool to 200°C at which time it was opened and the assembly removed.

B. Bond Evaluation

Low resistance bonds were consistently produced by this process. However, the bonds were often quite weak and separated under light pressure. The use of one inch long shoes tended to magnify this lack of strength since the shoes were easily grasped some distance from the elements.

In order to increase bond strength elements brazed with SnTe modified by the addition of one weight percent titanium were prepared by the techniques described above. Bond resistance was comparable to those obtained with SnTe brazed elements, almost always under 100 $\mu\Omega$.

Limited metallographic study has been made of bonded PbTe elements. The brittle nature of the material makes cutting and mounting difficult. Polishing and etching also present problems which are just beginning to be overcome. Figures 7a and 7b are photomicrographs of good bond areas in p-type and n-type PbTe respectively. In each case the shoe material is iron and the braze SnTe-Ti. A diffusion zone, about 0.005 inches wide is present in the n-PbTe sample, but absent in the p-material. More detailed studies are required to further define this anomoly.

A number of bonded elements were torque tested at room temperature, 315^{o} and 540^{o}C in the device pictured in Figure 3 (Chapter III). The results of these tests are given in Table 10. About one-half of the elements prepared for this test broke during handling prior to testing. Greater success was obtained with specimens brazed with SnTe-Ti. From Table 10 it can be clearly seen that the torque strength of n-PbTe elements is substantially greater than that of p-PbTe. Although the data is limited it appears that bonds made with SnTe-Ti may be stronger than those made with pure SnTe braze. It also appears that there is little, if any, effect of temperature.

The single test element made with p-PbTe - 1 w/o Mo was the strongest p-element tested at room temperature again indicating that further study of this material is warranted.

Examination of the fractured elements showed that the mode of failure was different in p-type and n-type materials. The p-PbTe almost always fractured in the thermoelectric material near the bond interface while the n-elements fractured at the bond. However, a chip often was removed from the n-elements and a crack along the surface at an angle near but less than 45^{o} was usually observed. These effects are discussed in detail in the chapter on stress analysis following.

Several specimens, also bonded with SnTe-Ti braze, were held at 538^{o}C for 113 hours and then torque tested. Bond resistance measurements showed that no appreciable change resulted from this treatment. Two p-elements and two n-elements broke after the thermal treatment, but before strength tests could be made. Results of these tests, which are reported in Table 11, were comparable to previous measurements. Fracture patterns were identical to those observed on samples not exposed to any thermal treatment. There was, however, a substantial increase in fracture strength of n-PbTe thermoelements. No such change was observed in p-PbTe. This is consistent with the conclusion, discussed in the following chapter, that p-PbTe of this diameter is cracked as a result of stresses resulting from the bonding process itself.

PbTe

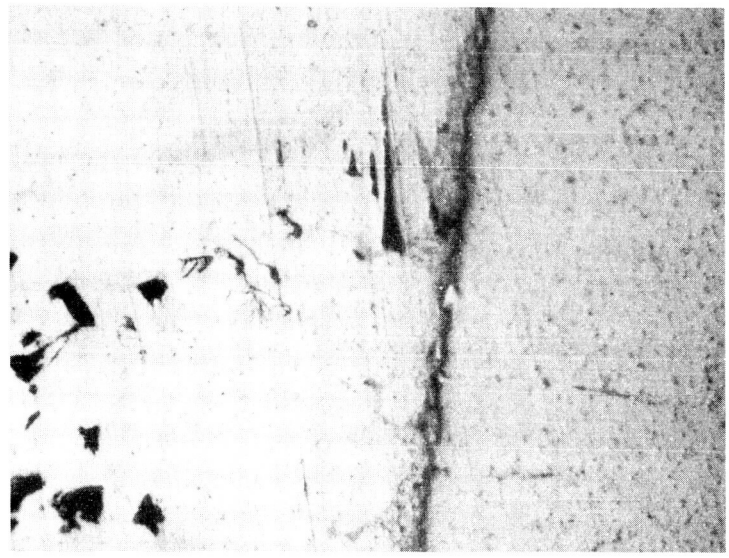

Fe

a) p-PbTe unetched 300X

PbTe

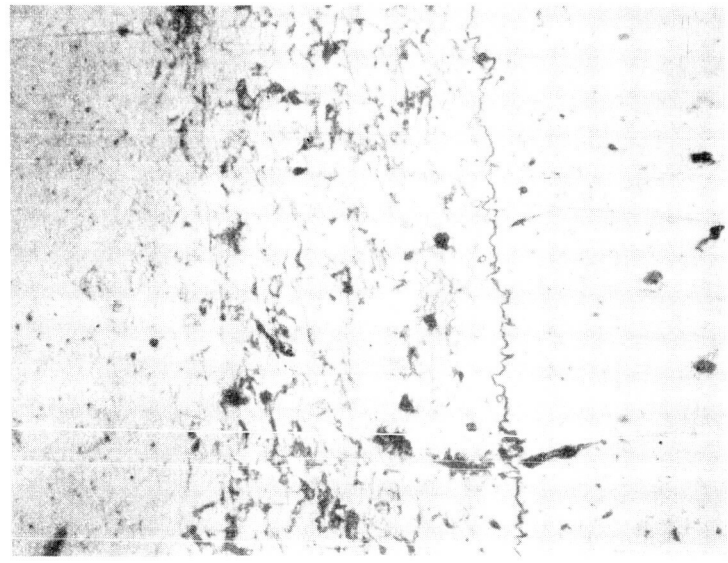

Fe

b) n-PbTe unetched 300X

Figure 7. PbTe Bonded to Iron Shoes with SnTe-Ti Braze

Table 10

Torque Test Results on Bonded Lead Telluride Thermoelectric Elements

Bond Test No.	Material	Braze	Bond Resistance $\mu\Omega$	Test Temp., °C	Torque Strength, psi	Comments
78	n-PbTe	SnTe	73, 0	25	100	Poor Bond
103	n-PbTe	SnTe-Ti	-- -	25	1100	Good Bond
104	n-PbTe	SnTe-Ti	19, 19	25	1250	Bond Only Fair Looking
114	n-PbTe	SnTe-Ti	75, 0	25	1275	Good Bond
95	p-PbTe	SnTe	132, 10	25	225	Little Wetting
105	p-PbTe	SnTe-Ti	58, 44	25	390	Broke in Element
106	p-PbTe	SnTe-Ti	52, 60	25	448	Broke in Element
134	p-PbTe + 1 w/o Mo	SnTe-Ti	75, 15	25	600	Broke in Element
87	p-PbTe	SnTe	30, 0	315	248	Broke in Element
88	p-PbTe	SnTe	6, 10	315	550	Broke in Element
93	p-PbTe	SnTe	20, 0	315	125	Poor Wetting
112	p-PbTe	SnTe-Ti	120, 80	315	625	Broke in Element
86	p-PbTe	SnTe	10, 0	540	248	Poor Wetting
90	p-PbTe	SnTe	0, 0	540	325	Good Bond - Broke in Element
91	p-PbTe	SnTe	90, 0	540	575	Broke in Element
107	p-PbTe	SnTe	175, 210	540	385	Broke in Element
115	p-PbTe	SnTe	80, 210	540	200	Broke in Element

Table 11

Torque Test Results on Bonded Lead Telluride Thermoelements Tested After 113 Hours at 538°C

Bond Test No.	Material	Braze	Bond Resistance, μΩ As Bonded	Bond Resistance, μΩ After 113 Hours at Temp.	Torque Strength, psi (25°C)
118	n-PbTe	SnTe-Ti	22; 110	30; 43	800
123	n-PbTe	SnTe-Ti	30; 45	48; 48	1700
126	n-PbTe	SnTe-Ti	0; 9	0; 44	1650
128	n-PbTe	SnTe-Ti	0; 45	35; 42	1800
121	p-PbTe	SnTe-Ti	37; 40	55; 72	500
124	p-PbTe	SnTe-Ti	25; 75	107; 122	350

VII. STRESS ANALYSIS

In this section we shall consider that the thermoelectric element is a brittle material and that, therefore, its failure criterion is that it fractures when the maximum principal stress reaches a limit, namely, the fracture stress. We shall assume that the thermoelement is a right circular cylinder with its length approximately twice its diameter. It is bonded to a shoe at each end. The shoes have the same dimensions as the thermoelement and are much stronger than the element so that yielding or fracture of the shoes need not be considered.

Three separate stress patterns can be identified. In general, two of these patterns may occur simultaneously, but not three. The patterns are, first, that caused by the axial temperature gradient in the element when it is operating, second, that caused by mechanical constraints imposed on the element by the shoe, and third, that created by the torque test used in this program. The first two are present during normal operation, and the second two are present during the torque test. These stress patterns will now be discussed in turn.

A. Thermal Gradient Stress Pattern

Let us first assume that the Seebeck coefficient, thermal conductivity, and electrical resistivity for the element are all constant with temperature, that radial heat flux is zero, and that heat is put into and removed from the element by radiation so that it is free from all external surface forces or constraints. Under these conditions the temperature gradient in the element exists in the axial direction only and it is a linear gradient. The element will assume the shape shown in Figure 8a and it will be free of all stresses, normal and shear. At first it may appear that shear stresses must exist because of the change in shape. The new shape is that defined by two concentric spheres and a right circular cone with its apex at the center of the spheres. The cylindrical coordinates of the original shape have now become spherical coordinates but remain mutually perpendicular at all points, indicating that shear is absent. The change in shape is due solely to the varying change in linear dimension along the temperature gradient and, as long as this gradient is linear, occurs without internal constraint.

Consideration of the geometry of Figure 8a leads in a straightforward manner to the following equations for the distortion of the element:

$$\beta = \frac{D_o}{L_o} \cdot \frac{\alpha (T_2 - T_1)}{1 + \alpha \left(\frac{T_2 + T_1}{2} - T_o \right)} \tag{1}$$

$$h \cong \frac{L_o}{\alpha (T_2 - T_1)} \left[1 - \cos \beta/2 \right] \tag{2}$$

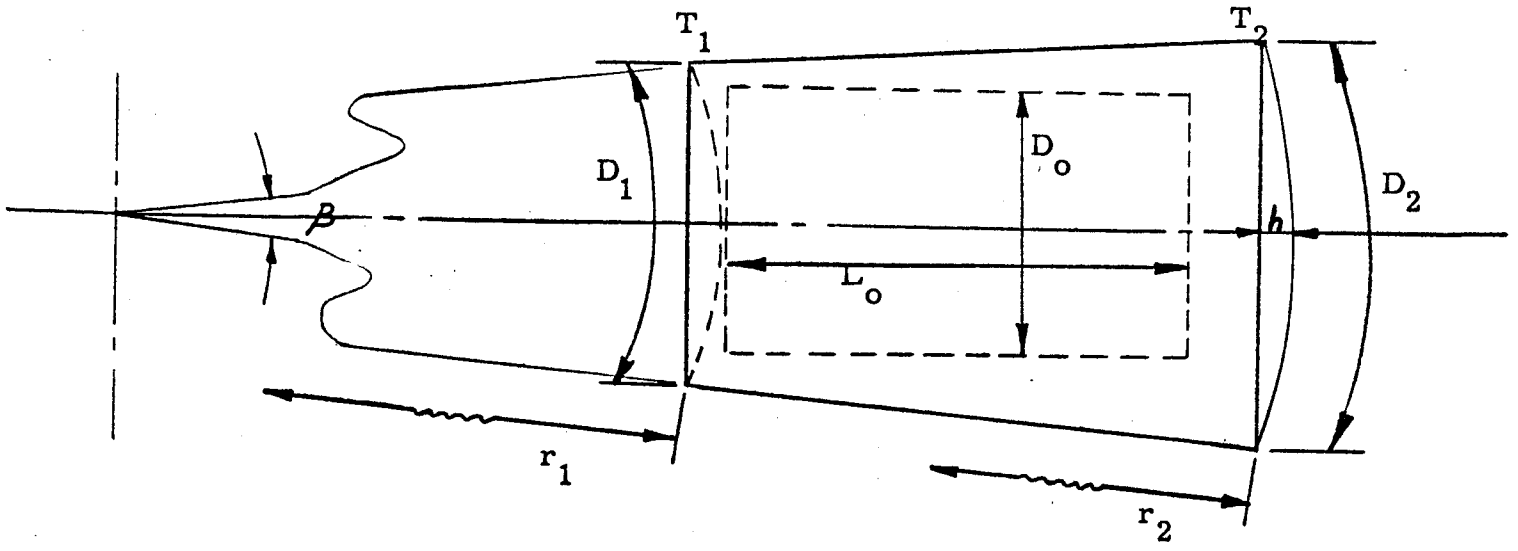

----- original shape at T_o

—— final shape under ΔT, $T_2 > T_1 > T_o$

Figure 8a

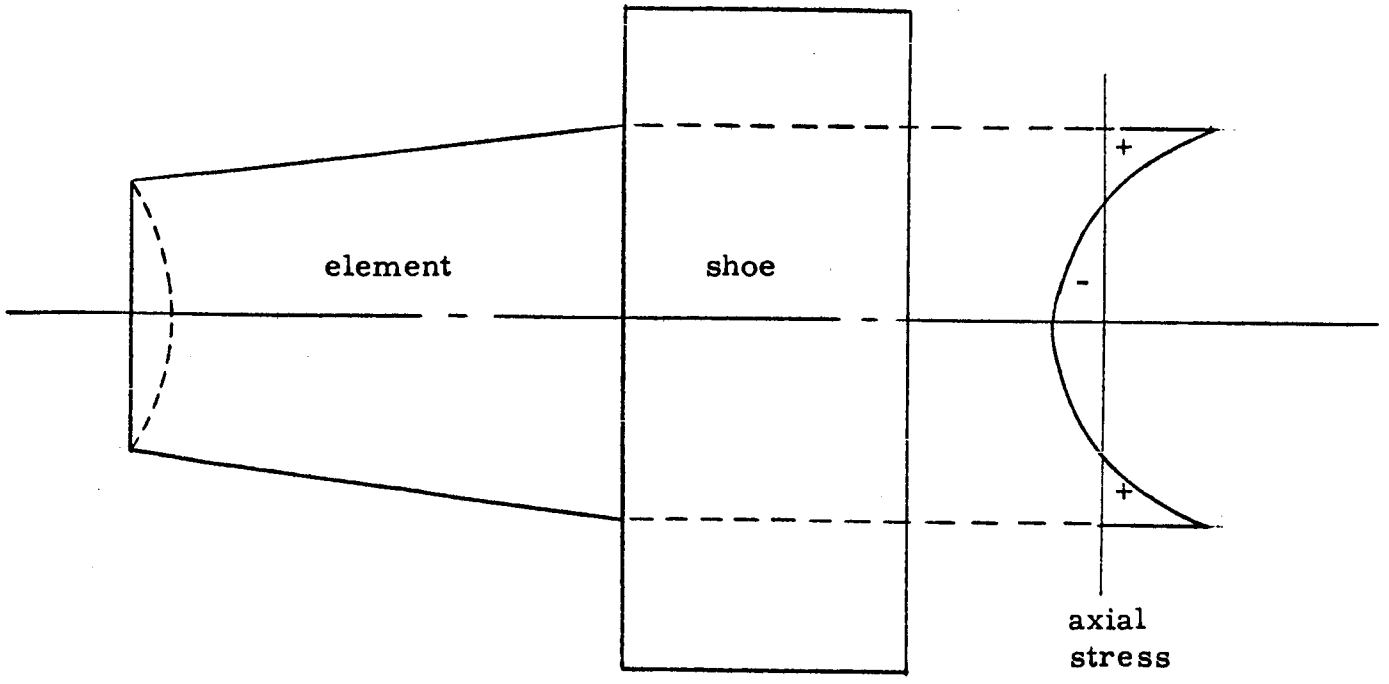

Figure 8b

Thermal Gradient Stress Patterns

where α is the coefficient of linear thermal expansion and the other terms are identified in Figure 8a.

In order to investigate the stresses occurring in a bonded element due to this effect alone, let us assume that the element is bonded at the hot end to a shoe having the same coefficient of thermal expansion as the element, a very high thermal conductivity, and having a large mass and a high Youngs Modulus. Under these conditions the element will be constrained axially so that its base is forced to become plane but it will not be constrained radially. The bonded element is shown in Figure 8b, which also indicates the distribution of axial stress at the bond plane. It is apparent that these stresses are the major ones present. The shoe applies compressive stresses to the element at the centerline and tensile stresses at the surface. Proceeding into the element from the shoe, these stresses eventually cancel each other with load transfer occurring through shearing stresses.

It is interesting to note that if a second shoe is bonded to the colder end, the axial forces will be reversed in sign, i.e., tensile on the centerline and compressive at the surface. If the element were quite short these axial stresses would tend to cancel each other but the associated shear stresses would be additive. This is indicative of the fact that long cylindrical elements will conform to the shoe by axial extensions while short wafer-like elements will conform by bending.

A complete stress analysis has not been performed but an approximate solution for the maximum axial stress has been obtained. The maximum axial displacement at the surface is:

$$\mu = \frac{h^2}{r_2 \sin^2 \beta/2} \tag{3}$$

If one assumes that the axial stresses are cancelled in 1/n of the element length the maximum stress, which we shall call σ_{grad}, for gradient stress. has the following value:

$$\sigma_{grad.} = \frac{n E h^2}{L_o r_2 \sin^2 \beta/2} \tag{4}$$

This stress has a value of 2250 psi under the following property values and dimensional assumptions:

E	=	2×10^6 psi
α	=	$18 \times 10^{-6}\ ^{o}C^{-1}$
D_o	=	0.5 inch
L_o	=	1.0 inch
T_2	=	$600^{o}C$

T_1 = $200^{\circ}C$

T_o = $0^{\circ}C$

n = 10

It is thus apparent that under the postulated conditions the gradient stress may approach the breaking stress of the element. The actual case will be less severe due to deformation of the shoe.

Two additional sources of thermal stress exist in an operating thermocouple but they are probably smaller than the above effect. First, the figure of merit of PbTe peaks rather sharply over the usual operating temperature range and second, radial heat flow is not zero. Both effects introduce nonlinearities into the thermal gradient and therefore introduce additional thermal stresses.

B. Shoe Constraint Stress Pattern

We will now consider the stresses that arise because of the difference in thermal expansion between the element and the shoe. If we consider the bond to be made by brazing, it is apparent that below the brazing temperature the component having the higher coefficient of expansion will be in tension and that the stress level will continuously increase as the bond temperature is lowered. Thus, in the normal functioning of a PbTe-Fe thermocouple, the element is in tension and the stresses are most severe at room temperature, relaxing appreciably as the bond is heated back toward the brazing temperature. If a brittle material were perfectly elastic up to its fracture stress it would not be subject to fatigue. Thus, if it did not fracture on the first application of maximum stress, it would survive all subsequent applications of the same stress. This is not strictly true for PbTe but probably represents a useful approximation over a limited number of cycles.

We will consider the case of an element formed by brazing together at T_B an element and a shoe each of which have a length to diameter ratio of 2.0. The shoe and the element are formed so that they will have the same diameter at T_B. The joint is formed and the bonded element is allowed to cool to some temperature, T. We shall consider only one end of the element and we shall not identify the shoe and the element, referring only to component #1 as having the larger coefficient of expansion and to component #2 as having the smaller. The results are thus applicable whether the element is #1 or #2. Conditions at temperature T are indicated in Figure 9a. The stress pattern in and near the joint is very complex and depends to an important extent on the properties of the braze material. Problems of this type are more readily investigated by experimental methods than by analysis. Nevertheless, appreciable information can be obtained short of a complete analytical solution.

The process by which the load is transferred from Side 1 to Side 2 through the braze is at the heart of the problem. Figures 9b and 9c are

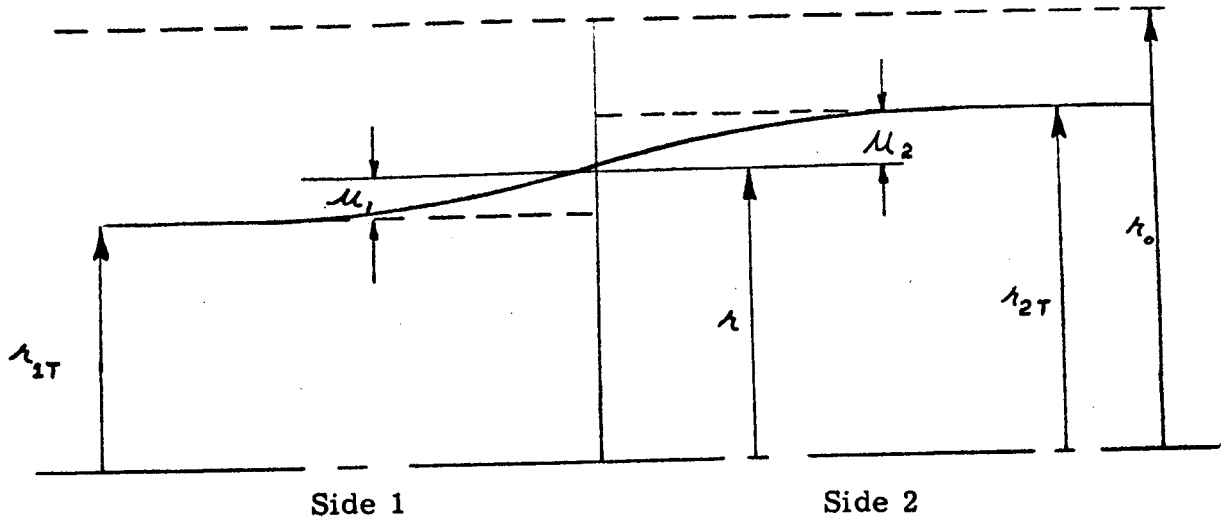

r_o = unstrained radii at T_B, brazing temperature

r_{1T} = radius side 1, unstrained at T, $T < T_B$

r_{2T} = radius side 2, unstrained at T

r = radius of bond, strained, at T

Figure 9a

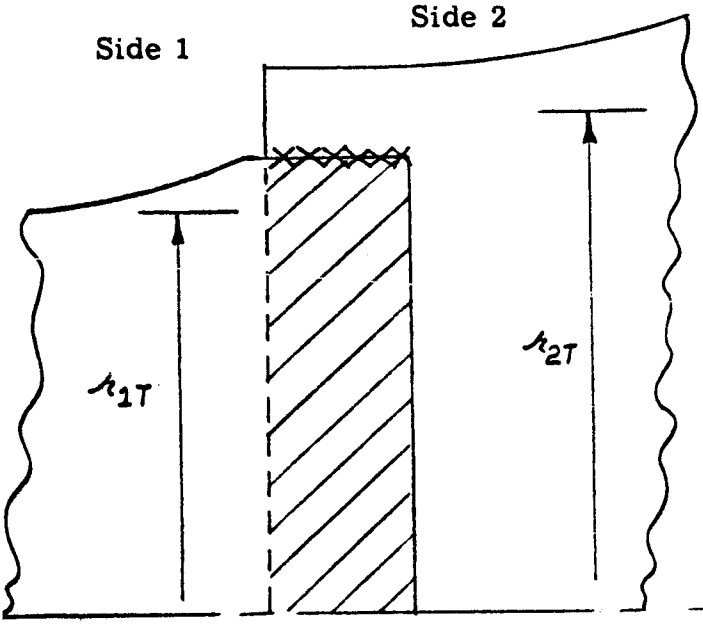

Figure 9b

Tensile Braze Joint

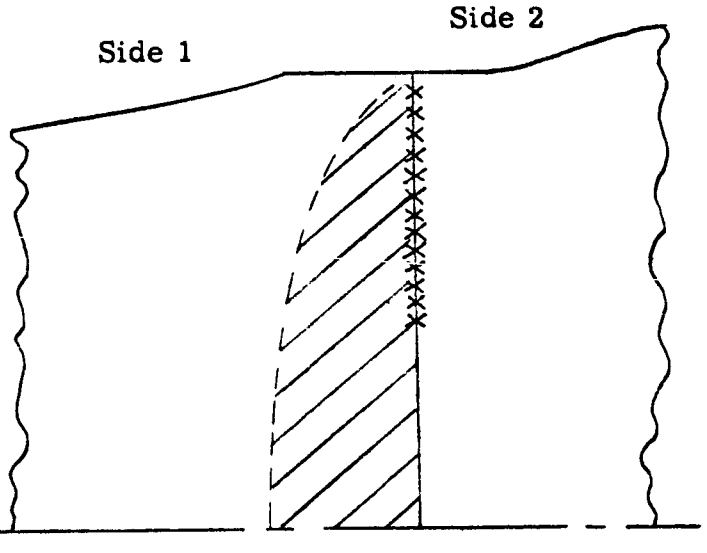

Figure 9c

Shear Braze Joint

presented to clarify the process. In Figure 9b Side 2 has been enlarged and extended around Side 1 and the braze is confined to the periphery, neglecting for the moment, the problem of heat transfer. Under these conditions, the stress pattern in Side 1 is relatively simple. Within the cross hatched area the radial and tangential stresses tend to be equal and constant and shear to be zero, modified by the effect of the balance of the cylinder. The use of a braze joint loaded in shear, as indicated in Figure 9c, may be a structural simplification, but it is a very imperfect substitute for the other construction when the complexity of the resulting stresses is considered. Side 2 is now poorly located to load Side 1 uniformly and the biaxial stress pattern develops only gradually as the loads are transferred into Side 1 by shear stresses. The shear stress in the braze is non-uniform. The load is distributed over an annular region of the bond only by yielding of the braze at the periphery. The load in the braze falls toward zero from the periphery inward and in many cases probably reaches zero. The cross-hatched zone in Figure 9c indicates the gradual development of the zone of biaxial tension which is uniform in the other case. If the braze did not possess sufficient ductility to yield at its periphery, thus distributing the load over a larger area it would inevitably fail. The zone in Figure 9c in which the biaxial tension condition is developing is subjected to shear stresses. The detailed nature of this local stress pattern is controlled by the manner in which the braze joint adjusts to the load and is, in general, not readily calculable.

In order to obtain a feeling for the general range of stresses involved, we will assume a condition of plane stress in the Figure 9b situation. This leads to the following results for r, the radius of the bonded interface, and for σ_{shoe}, the maximum tensile stress caused by shoe constraint.

$$r = r_o \left[\alpha_1^* + \frac{E_2^* (\alpha_2^* - \alpha_1^*)}{E_2^* - E_1^*} \right] \tag{5}$$

$$\sigma_{shoe} = \frac{E_1^* E_2^* (\alpha_2^* - \alpha_1^*)}{\alpha_1^* (E_2^* - E_1^*) + E_2^* (\alpha_2^* - \alpha_1^*)} \tag{6}$$

where, with subscripts 1 or 2,

α_i^* = $1 + \alpha_i (T - T_B)$

E_i^* = $\frac{E_i}{1 - \nu_i}$

α = linear coefficient of thermal expansion

E = Young's modulus

ν = Poisson's ratio

A value of σ_{shoe} has been calculated for a representative set of values. It was found to be 17,700 psi when:

R_o = 0.25 inch
α_1 = $18 \times 10^{-6}\ ^oC^{-1}$
α_2 = $10 \times 10^{-6}\ ^oC^{-1}$
E_1 = 2×10^6 psi
E_2 = 30×10^6 psi
ν_1 = 0.20
ν_2 = 0.28
T_B = 700^oC
T = 0^oC

The fact that σ_{shoe} is appreciably greater than σ_{grad} implies that shoe constraint effects are more serious than those due to thermal gradients. The value of 17,700 psi is well above the fracture strength of PbTe. The discrepancy can be explained only in part by the simplified model used because even in the situation of Figure 9c, the stress should closely approximate the simpler case along and near the axis. Flow of the braze during the earlier stages of cooling may reduce the stresses somewhat but this is not a complete explanation since in Equation (6) the relation between σ and ΔT is close to linear and ΔT would have to be reduced to 200^oC or less to bring σ_{shoe} down to measured strength levels of PbTe. The explanation probably does lie in the braze behavior however. In the situation of Figure 9c, if the braze flows sufficiently to permit significant offsetting of Side 1 from Side 2, the stresses will be greatly reduced. Since the total calculated elastic elongation of the PbTe radius is only 0.0016 inch, the total strain could be relieved by offsetting without being particularly noticeable.

It should be mentioned that there is a small axial stress component present as well. As can be noted in Figure 9a, the axial fibers at the surface are elongated somewhat relative to those at the centerline. This will result in an axial stress component, tensile at the surface and compressive at the centerline. These stresses will be much smaller than the radial-tangential stresses previously discussed.

The biaxial stress pattern will cause a brittle material to fracture in a series of cracks originating at or near the bond and extending into the brittle leg in planes parallel to the axis but randomly located around the axis. The cracks will tend to stop when they have progressed out of the highly stressed region. Their orientation is not such as to cause ready separation of the joint, or even to interfere markedly with electrical and thermal conductivity parallel to the axis.

C. Torsional Stress Pattern

In order to investigate the behavior of bonded joints further, a series of torsional tests were performed. The torsional stress pattern is simple and well known and is shown in Figure 10. It consists of a state of pure shear on all cylindrical surfaces falling from a maximum on the surface to zero at the centerline. The stress pattern is constant as a function of axial displacement. Its value is:

$$\tau_{z\theta\,(MAX.)} = \sigma_1 = \frac{16M}{\pi D_o^3}$$

Brittle materials characteristically fracture in torsion under the action of σ_1 in a 45° helical pattern. If the end loads are applied without stress concentration, the location of the initial fracture site should be random along the cylindrical surface. In the present case, when M is applied through two bonded shoes, the torque stress pattern is complicated by shoe constraint stresses at the ends and fracture can be expected to initiate in the thermoelement adjacent to the bond.

D. Experimental Program

A series of torque tests were performed on p- and n-elements bonded at each end to iron shoes. The braze in each case was SnTe or Ti modified SnTe and the brazing temperature was 790 - 800°C. All samples were 0.5 inch in diameter. Tests were run at room temperature, 315°C, and 540°C. Results are tabulated in Tables 10 and 11 in Chapter VI. It can be noted from the data first, that temperature does not exert a strong influence in this range and second, that the n-elements are characteristically about two to three times as strong as the p-elements, failing at 1100-1300 psi while the p-elements fail at 380 ± 200 psi.

One further highly significant observation can be made from the samples and is indicated in Figure 11, a photograph of characteristic fractures of p- and n-elements and Figure 12 which shows the helical crack pattern in an n-PbTe element which did not break. The p-type fractures characteristically resulted in the creation of a significant number of loose shards with a portion of the element still attached to the shoe. The fracture surface as revealed by the remnants adhering to the shoe was generally symetrical with the axis. The n-type fractures frequently appeared at first inspection to represent a clean shear cleavage in the braze in that no significant quantity of element was left adherent to the shoe. On closer inspection, however, it was noted that in many cases a small chip had fallen from the element as shown in Figure 11 and the 45° helical crack pattern was clearly evident. In almost all samples a pronounced 45° helical crack could be observed even though no chip had fallen out.

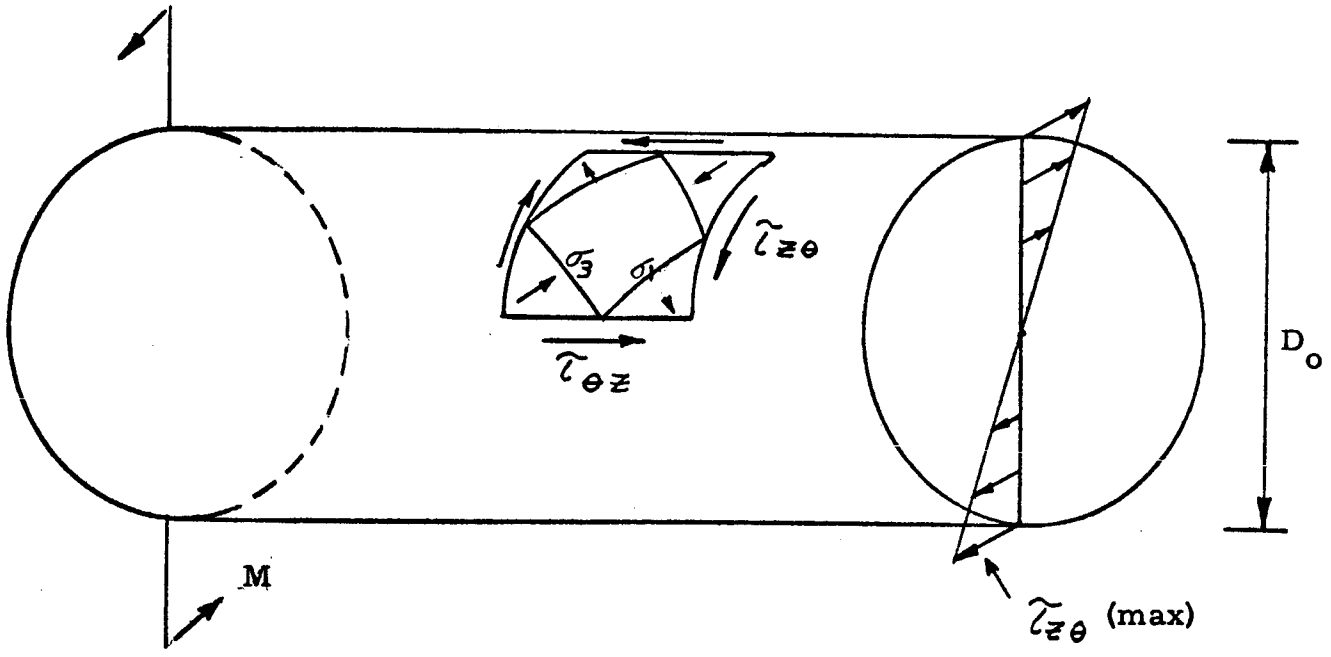

Figure 10

Torsional Stress Pattern

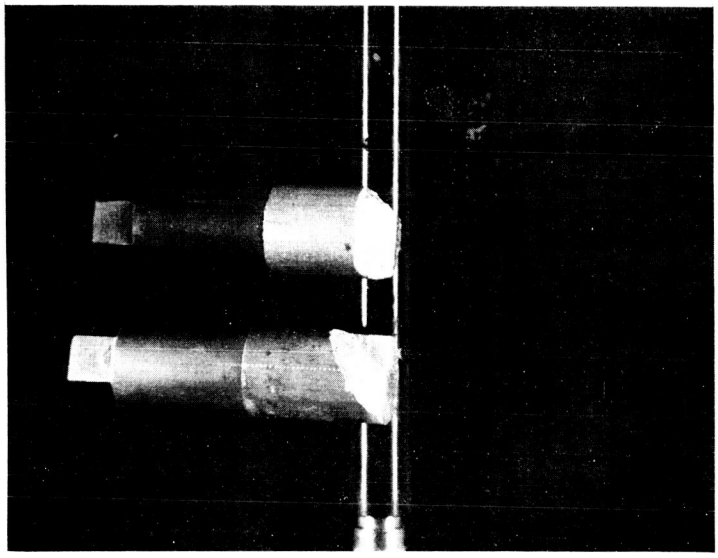

Figure 11. PbTe Thermoelements Fractured in Torsion

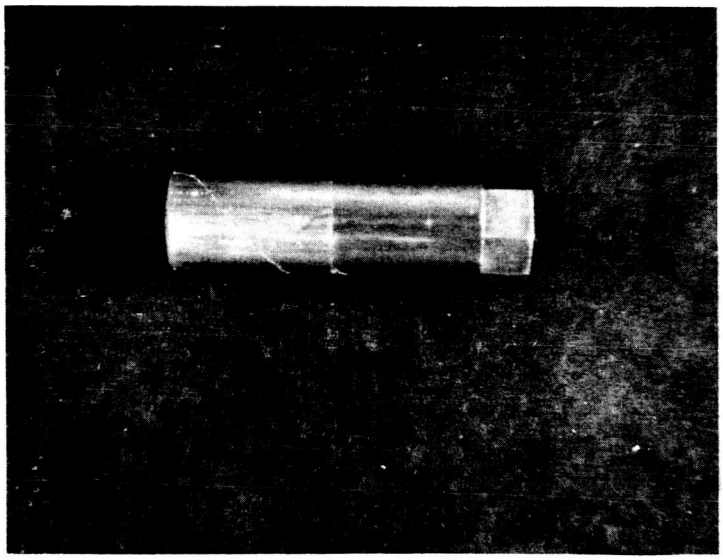

Figure 12. n-PbTe Thermoelement Tested in Torsion
(note helical crack)

These results can be interpreted in the following way. First, it must be recognized that the stress calculated from the torque at fracture does not represent the true facture strength of the material. This is so because a significant component of σ_{shoe} was also present and fracture actually occurred under the combined action of the torque and the shoe constraint loads. This is verified by the fact that fracture invariably occurred near the bond interface. The consistent helical pattern of fracture of the n-type elements indicates that the torque stress is controlling the fracture. Careful examination of the fractures indicated that the helical angle at the interface, where the crack initiated, is actually less than 45^{o}, being approximately 35^{o} relative to the axial direction, indicating that an appreciable component of tangential stress is present and aiding in the fracture.

The p-type fractures strongly suggest that prior cracking had occurred under the action of σ_{shoe}. This is indicated primarily by the non-helical fracture and by the tendency of numerous loose shards to fall from the fracture. Thus, the true reason for the low torque strength of the p-elements is the fact that the element was not strong enough to induce flow in the braze during cooling but instead cracked locally under the applied loads. The subsequently applied torque merely extended existing cracks.

In conclusion, the above analysis has provided an indication of the relative importance of temperature gradient and shoe constraint stresses and has provided equations by which the relative stress levels in various combinations of element and shoe can be calculated. It has also indicated the strong influence that the braze material exerts on the stress patterns. The postulated cracks in the p-elements could be eliminated by use of a sufficiently soft braze or by use of a shoe material having a close match in expansivity.

VIII. REFERENCES

1. E. Brady, et al, Thermoelectric Materials and Fabrication, Final Report on Contract NObs-84776, Report No. GA-3754, February 1963.

2. Thermoelectricity, Final Report by Westinghouse Electric Corporation on Contract NObs-86595, January - December 1963.

3. Module Improvement Program, Final Report by Westinghouse Electric Corporation on Contract NObs-84329, August 31, 1962.

4. Martin Company, Personal Communication.

5. Power Dense Thermoelectric Module, Interim Report, 3 July 1961 - 2 November 1962, Prepared by Tyco Laboratories, Inc. on Contract NObs-86538, March 1, 1963.

6. Thermoelectric Power Generation, Quarterly Report No. 5, Prepared by General Electric, Direct Energy Conversion Operation under Contract NObs-86854, May 15, 1963.

7. Thermoelectric Power Generation, Final Report, Prepared by General Electric, Direct Energy Conversion Operation under Contract NObs-86854, December 10, 1963.

8. Fabrication Technique Development, In-Line Thermoelectric Generator Modules, prepared by General Instrument Corporation on Contract NObs-86538, March 1, 1963.

9. Thermoelectric Generator Element - Type TEGS-3P, 3M Company Brochure (no date).

10. Thermoelectric Bonding Study, The Bonding of PbTe and PbTe-SnTe with Non-Magnetic Electrodes, Prepared by Tyco Laboratories under Contract NAS5-3986, September 1964.

11. W. T. Hicks and H. Valdsaar, High Temperature Thermoelectric Generator, Quarterly Report, June 13 to September 30, 1963, prepared by DuPont on Contract NObs-88639.

APPENDIX A

I. THERMAL GRADIENT STRESS PATTERN

Referring to Figure 8a:

Considering thermal expansion

$$D_1 = D_o \left[1 + \alpha (T_1 - T_o)\right]$$

$$D_2 = D_o \left[1 + \alpha (T_2 - T_o)\right]$$

where α = coefficient of linear thermal expansion.

$$\beta = D_1/r_1 = D_2/r_2$$

hence:

$$r_2 - r_1 = \frac{D_2 - D_1}{\beta}$$

$$\beta = \frac{D_2 - D_1}{r_2 - r_1}$$

But again considering thermal expansion:

$$r_2 - r_1 = L_o \left[1 + \alpha \left(\frac{T_1 + T_2}{2} - T_o\right)\right]$$

Substituting:

$$\beta = \frac{D_o}{L_o} \frac{\left[1 + \alpha (T_2 - T_o)\right] - \left[1 + \alpha (T_1 - T_o)\right]}{\left[1 + \alpha \left(\frac{T_1 + T_2}{2} - T_o\right)\right]}$$

or

$$\beta = \frac{D_o}{L_o} \frac{\alpha (T_2 - T_1)}{\left[1 + \alpha \left(\frac{T_1 + T_2}{2} - T_o\right)\right]}$$

which is Equation (1) in the text.

From Figure 8a:

$$\cos \beta/2 = \frac{r_2 - h}{r_2}$$

$$h = r_2 (1 - \cos \beta/2)$$

$$r_2 = \frac{D_2}{\beta}$$

substituting:

$$r_2 = L_o \frac{\left[1 + \alpha (T_2 - T_o)\right]\left[1 + \alpha \left(\frac{T_1 + T_2}{2} - T_o\right)\right]}{\alpha (T_2 - T_1)}$$

since, in cases of interest:

$$\alpha \approx 18 \times 10^{-6}, \quad \Delta T \approx 5 \times 10^2$$

$$r_2 \approx \frac{L_o}{\alpha (T_2 - T_1)}$$

$$h \approx \frac{L_o}{\alpha (T_2 - T_1)} (1 - \cos \beta/2)$$

which is Equation (2) in the text.

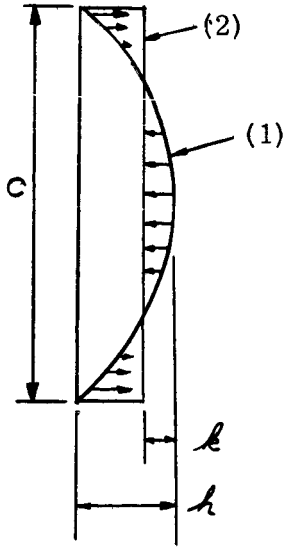

The hot end of the element is shown in the unconstrained shape, (1) and the constrained shape, (2). The point of stress inflexion is determined by the condition that the net axial force be zero. To a reasonable approximation, the deformation diagram is equivalent to a force diagram if the deformations are multiplied by Young's modulus and hence the point of inflexion is approximately located by the condition that the spherical segment of height k is equal in volume to the annular volume defined by the tensile stresses, or:

$$\frac{\pi}{4} C^2 (h - \ell) = \frac{\pi}{3} h^2 (3r_2 - h)$$

since $C = 2r_2 \sin \beta/2$

$$(h - k) = \frac{h^2 (3r - h)}{3r_2^2 \sin^2 \beta/2}$$

however: $3 r_2 >>> h$, hence

$$h - k \simeq \frac{h^2}{r_2 \sin^2 \beta/2}$$

(h - k) is the maximum tensile deformation in the outermost fibers. If L_o/n is the actual gage length over which this deformation occurs, the maximum stress is:

$$\sigma_{MAX.} = E \frac{n}{L_o} \frac{h^2}{r_2 \sin^2 \beta/2}$$

which is Equation (3) in the text. It seems likely that n will have a value of the order of 10.

II. SHOE CONSTRAINT STRESS PATTERN

The solution is based upon the assumption of plane stress near the interface with the loads applied only at the periphery. The load is +P on Side 1 and -P on Side 2. The stress pattern is then defined as:

$$\sigma_r = \sigma_\theta = P$$

$$\sigma_z = 0 ; \quad \text{all} \quad \tau = 0 \qquad (1)$$

With regard to strains:

$$\varepsilon_r = \frac{d u}{d r} \qquad (2)$$

$$\varepsilon_\theta = \frac{u}{r} \qquad (3)$$

where u is total radial displacement.

The pertinent stress-strain relationships are:

$$\varepsilon_r = \frac{1}{E} (\sigma_r - \nu \sigma_\theta) \qquad (4)$$

$$\varepsilon_\theta = E (\sigma_\theta - \nu \sigma_r) \qquad (5)$$

Substituting (1) into (4) and (5);

$$\varepsilon_r = \frac{P}{E}(1-\nu) = \varepsilon_\theta \tag{6}$$

From (3) and (6):

$$u = \frac{1}{E} P r (1-\nu) \tag{7}$$

$$P = \frac{u E}{r (1-\nu)} \tag{8}$$

Let $E^* = \frac{E}{1-\nu}$

$$P = \frac{u}{r} E^* \tag{9}$$

From balance of forces on opposite sides:

$$\frac{u_1}{r} E_1^* = - \frac{u_2}{r} E_2^* \tag{10}$$

$$\frac{1}{r}\left[u_1 E_1^* + u_2 E_2^*\right] = 0 \tag{11}$$

r is defined by the condition that the quantity in the bracket is zero, since 1/4 is not. Hence:

$$u_1 E_1^* = - u_2 E_2^* \tag{12}$$

Referring to Figure 9a:

$$r = r_{1T} + u_1 = r_{2T} - u_2 \tag{13}$$

$$u_1 = r_{2T} - r_{1T} - u_2 \tag{14}$$

$$\mu_2 = r_{2T} - r_{1T} - \mu_1 \tag{15}$$

From consideration of thermal expansion:

$$r_{1T} = r_0 \left(1 + \alpha_1 (T - T_B)\right) \tag{16}$$

$$r_{2T} = r_0 \left(1 + \alpha_2 (T - T_B)\right) \tag{17}$$

Let $\alpha^* = \left(1 + \alpha (T - T_B)\right)$. Combining (12), (15), (16), (17):

$$\mu_1 E_1^* = -E_2^* \left[r_0 (\alpha_2^* - \alpha_1^*) - \mu_1 \right] \tag{18}$$

$$\mu_1 = r_0 \frac{E_2^* (\alpha_2^* - \alpha_1^*)}{E_2^* - E_1^*} \tag{19}$$

Similarly:

$$\mu_2 = r_0 \frac{E_1^* (\alpha_2^* - \alpha_1^*)}{E_1^* - E_2^*} \tag{20}$$

From (13), (16), (19):

$$r = r_0 \left[\alpha_1^* + \frac{E_2^* (\alpha_2^* - \alpha_1^*)}{E_2^* - E_1^*} \right] \tag{21}$$

which is Equation (5) in the text.

From (1), (9), (21):

$$\sigma = \frac{\tau_o E_1^* \dfrac{E_2^*(\alpha_2^* - \alpha_1^*)}{E_2^* - E_1^*}}{\tau_o \left[\alpha_1^* + \dfrac{E_2^*(\alpha_2^* - \alpha_1^*)}{E_2^* - E_1^*}\right]} \tag{22}$$

which leads directly to Equation (6) in the text.

$$\sigma = \frac{E_1^* E_2^* (\alpha_2^* - \alpha_1^*)}{\alpha_1^* (E_2^* - E_1^*) + E_2^* (\alpha_2^* - \alpha_1^*)} \tag{23}$$